

ALMA MATER STUDIORUM · UNIVERSITÀ DI BOLOGNA

Scuola di Scienze

Dipartimento di Fisica e Astronomia

Corso di Laurea Magistrale in Fisica del Sistema Terra

**Analytical solutions for the run-up of long
water waves excited by time-independent
and time-dependent forcing**

Relatore:

Prof. Alberto Armigliato

Presentata da:

Cesare Angeli

Anno Accademico 2019/2020

Abstract

Nello studio fisico e matematico dei maremoti, l'interazione con la costa, detto anche problema del *run-up* rappresenta ancora oggi una grande sfida. Da un lato, si tratta forse del problema di maggiore urgenza, in quanto è proprio all'arrivo alla terra ferma che il maremoto causa le maggiori perdite, sia in termini di vite umane che di infrastrutture. Dall'altro lato, la formulazione matematica del problema è particolarmente complessa ed alcune caratteristiche del fenomeno non sono ancora ben comprese.

In questa tesi viene proposto un metodo di calcolo della posizione della linea di costa in problemi bidimensionali, che suppone di poter applicare le equazioni della fluidodinamica in approssimazione di *shallow water* e linearizzate. Se la prima di queste ipotesi è sempre utilizzata in questo contesto, questo non vale per la seconda. In generale il problema è non lineare e prevede condizioni al contorno mobili. Nonostante ciò, si può notare un fatto sorprendente: i problemi ai valori iniziali in formulazione lineare e non lineare producono soluzioni con gli stessi punti stazionari. Spesso l'informazione fondamentale che si vuole ottenere è l'estensione dell'area inondata, ovvero il valore massimo del *run-up*, che sarà previsto quindi correttamente anche in approssimazione lineare.

Sulla base di queste considerazioni, viene presentato un modello capace di prevedere l'inondazione su una spiaggia lineare dovuta ad una qualsiasi deformazione del fondale che sia piccola rispetto alla profondità locale del mare. Questo modello è quindi applicabile nel caso di terremoti e frane sottomarine in prossimità della costa.

I risultati delle applicazioni sono in accordo con i principali studi analoghi presenti in letteratura. Per questo, il modello è utilizzato per alcuni casi nuovi, ovvero uno studio della dipendenza del run-up massimo dalla magnitudo, in cui le caratteristiche della faglia sono dedotte da leggi di scala, e un nuovo semplice modello per una frana di forma Gaussiana con parametri variabili nel tempo.

Contents

Introduction	1
1 Phenomenology and Physics of Tsunamis	5
1.1 Tsunami as a 3-step process	6
1.2 A brief overview of the tsunami hazard and early warning topics	13
1.3 Tsunami run-up from an analytical point of view	19
2 Shallow Water Theory	21
2.1 Basic Fluid Dynamics	21
2.2 Scaling analysis and perturbative expansion	24
2.3 The shallow water approximation	27
2.4 A General Solution for a Uniformly Sloping Ocean	30
3 Analytical Approaches to Run-Up Calculations	35
3.1 Carrier & Greenspan Transformation	36
3.2 Maximum run-up from nonlinear and linear solutions	39
3.3 Linear solution for a fourier-series bottom excitation	41
4 Applications to Tsunamigenic Earthquakes	47
4.1 Tectonic tsunamis	47
4.2 Tsunami run-up dependence on the earthquake source	55

5 Applications to Tsunamigenic Landslides	63
5.1 Analytical landslide dynamics	63
5.2 Gaussian-shaped Solid Block	66
5.3 A Hint on landslides with time-dependent shape	68
Conclusion	75
Appendix A - Notes for the Numerical Implementation of the Solution	77
References	81

Introduction

Tsunamis represent a serious threat for human settlements and the awareness of this hazard has grown in recent years due to many destructive events, such as the Sumatra event in 2004 and the Tohoku-Oki event in 2011. Following these events, the global effort to prevent further casualties has grown. Obviously, this requires a great knowledge of the physical and mathematical aspects of the problem.

The process of a tsunami can be roughly described as a three phases problem. The first phase is the generation, where a large portion of the ocean surface is displaced, usually due to faulting events or mass wasting phenomena. The second phase is the propagation of the surface disturbance, for which the theory of long waves is commonly used. The third phase is the interaction with the coast, or *run-up*. This phase is obviously the most impactful, since it describes the evolution of the waves when they approach the coasts and can impact human settlements. Despite this, it is probably the least understood part of the process.

The study of the run-up of long waves for tsunami applications can be traced back to the pioneering work of Carrier & Greenspan (1958), who studied the evolution of long waves over a linearly sloping beach in two dimension. This setting has remained the most commonly used for the following studies and generalizations. The problem presents strong nonlinearities: not only the equations of fluid dynamics are nonlinear, but, since the interest is in the motion of the shoreline, the boundaries are time-dependent.

It has been observed though that the linear theory might be of great interest for the run-up problems. By solving the initial value problem in both the linear and nonlinear

formulation, it is possible to see that the predicted solutions have the same stationary points. Given the fact that the maximum horizontal extent of the inundated area is given by the maximum height reached by the shoreline, it can be correctly predicted by the linear theory. This fact encourages the use of linear theory for its simplicity and its greater flexibility for generalizations, but it has to be noted that other variables, such as the shoreline velocity or the energy density transported by the wave, need the nonlinear formulation. In this work, we decided to make use of the linear formulation to compute the shoreline position as a function of time.

Chapter 1 starts with the description of some basic facts about the phenomenology of tsunamis, namely the possible generation mechanisms and propagation properties, some hints about the probabilistic tsunami hazard assessment and it ends with a brief summary of the most relevant analytical studies concerning the run-up problem.

In chapter 2, the foundations of the theory are laid out. Starting from the equations of fluid mechanics in their inviscid form, the shallow water approximation is developed. Among the possible approaches, the one used here is especially intuitive in the case of waves produced by displacement of the ocean bottom and it is therefore suitable for the case of underwater landslides and faulting events. After this, a general solution for wave evolution over a linearly sloping beach is presented.

Chapter 3 deals specifically with the run-up problem. Firstly, a nonlinear solution for the initial value problem is presented, following the solution developed by Carrier et al. (2003). Then, the equivalence of this solution and the linear one for the prediction of stationary points is proved. This equivalence is used to argue in favor of the linear solution, since it can be generalized more easily, in particular in the case of time-dependent bottom displacement. Using the solution developed in chapter 2, it is shown that a simple analytical solution for the shoreline motion can be found by writing the bottom displacement as a superposition of sinusoidal functions with time-dependent coefficients.

In chapter 4 and 5, this solution is applied to analytical models for earthquake and landslides. For earthquakes, the bottom displacement is assumed to be instantaneous

and it is computed using a 2D plane-strain formulation of the widely used Okada (1985) model. This model assumes the fault to be in a homogeneous half-space and it is used here in the particular case of a dip-slip fault parallel to the coast, since it is the case that produces the biggest vertical displacement. As for landslides, it is at first assumed that the sliding body can be described as a solid block of Gaussian form. As an example of the generality of the problem, a new simple model of a Gaussian landslide with time varying parameters is briefly studied.

Chapter 1

Phenomenology and Physics of Tsunamis

Among the possible natural disasters, tsunamis are in a peculiar situation, since their occurrence is something virtually everyone is aware of and yet they still are extremely challenging for scientists and engineers. It is easy to understand this collective awareness: in both historical and recent memory, there have been catastrophic events that left a mark on the population. Just in the last two decades, the world has experienced, among others, the tsunami following the Indian Ocean earthquake on December 26th 2004, that caused more than 230000 casualties, the one caused by the Tohoku earthquake on March 11th 2011, which caused the meltdown at three reactors at the Fukushima Daiichi Nuclear Power Plant, and the Sulawesi event on September 28th 2018, the characteristics of which are still debated due to the complex geomorphological phenomena that accompanied the earthquake.

From just these few examples, it may be clear what factors make the situation so complicated:

- tsunamis are rare enough to prevent a purely phenomenological or statistical treatment of the hazard, but still frequent enough to represent a constant threat for

coastal settlements all around the world;

- they depend on a large number of parameters, ranging from bathymetric profiles and geomorphological properties of both the area where they originate and the coasts where they impact to the properties and characteristics of their causes;
- their causes are themselves rare and complicated events, such as great earthquakes or big mass movements.

Despite these difficulties, much progress has been made in the last decades, thanks to a deeper understanding of the physical processes involved, of the numerical codes used to simulate them, of the physical models in the lab and to the enhancement of the experimental measurements. For the latter, many instrumental techniques, e.g. data from oceanographic satellite missions and offshore/coastal tide gauges, are combined with the study of the source, usually represented by seismic recording of the earthquake, and routine in situ surveys of the coastal impact¹.

1.1 Tsunami as a 3-step process

The study of tsunamis is usually divided into three distinct parts, that follow the evolution of the process, namely the *generation* of the waves, their *propagation* across open ocean and the *run-up*, i.e. their evolution once they approach the shoreline.

Generation of tsunami waves. To cause a tsunami, there has to be a significant displacement of the entire water column, hence including the sea surface, from the configuration at rest. The most common mechanism is due to earthquakes. If a faulting event occurs in a sea area, the coseismic displacements of the sea bottom are transmitted

¹For the following part of the chapter, many general information about tsunamis will be given for granted. Whenever no explicit reference in literature is reported, it is intended that a general text about tsunamis, such as the ones by Levin (2016) or Saito (2019), or about fluid mechanics, as Kundu, Cohen & Dowling (2015), may be sufficient.

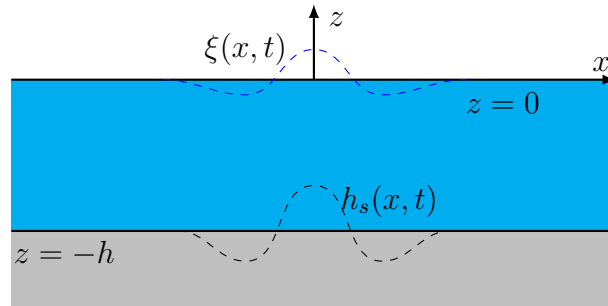


Figure 1.1: *Schematic representation of a tectonic tsunamigenic event. The ocean bottom and the free surface are represented respectively by the curves $z = -h$ and $z = 0$. At a given time, the ocean bottom undergoes a sudden deformation $h_s(x, t)$ that is transmitted to the free surface causing a displacements $\xi(x, t)$.*

to the free surface, generating the initial waveform that then propagates, as schematically shown in Fig. fig:generation. For this reason, it is evident that not every submarine earthquake can cause a tsunami: the most favourable case is that of thrusting events (as is the case for the Sumatra and the Tohoku events), but tsunamis have been observed also for other focal mechanisms (the Sulawesi earthquake was due to a strike-slip fault).

The second most common cause of tsunami generation is the interaction of landslides with a water body. Despite the great variety of this kind of events, there are mainly two scenarios:

- a submarine landslide is put in motion and it produces waves dynamically;
- a subaerial landslide falls into water at high speed. The falling body causes an impulsive forcing on the fluid surface and a dynamical forcing due to the portion that subsequently continues to move underwater.

It should be pointed out that landslides can originate from pure gravitational instability, but they can also be triggered by seismic loading. This factor has to be taken into account when studying the possible tsunami scenarios and in the reconstruction of

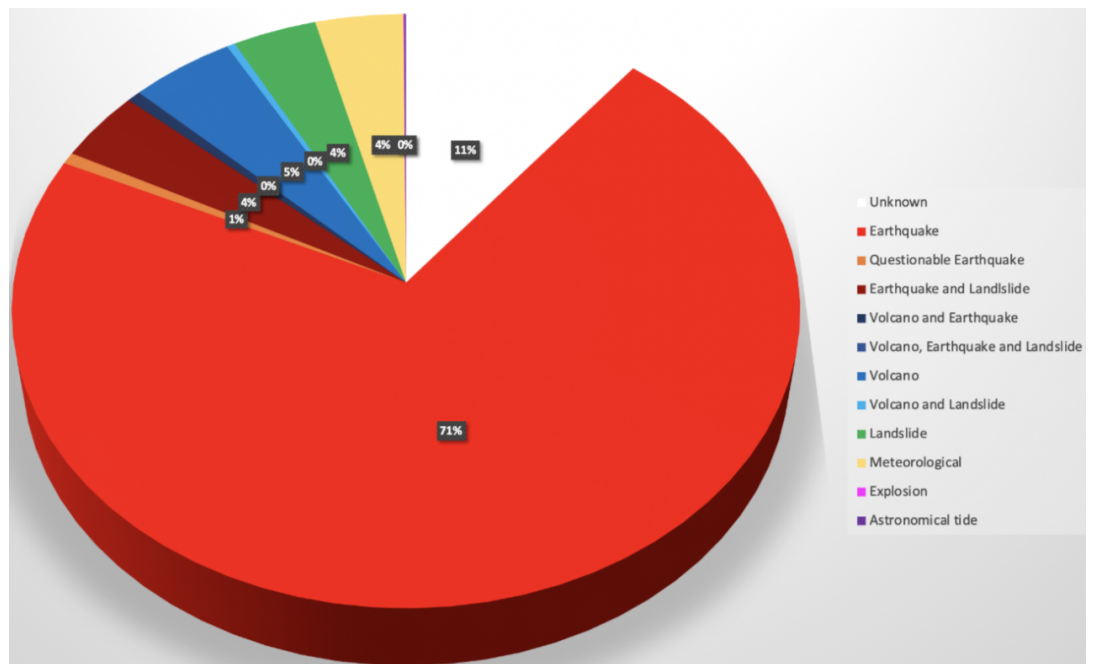


Figure 1.2: *Relative frequency of possible tsunamigenic sources plotted from data available from the National Geophysical Data Center (<https://www.ngdc.noaa.gov/>).*

historical events.

Another possible cause may be volcanic activity. So called *volcano tsunami* are usually caused by explosive eruptions, e.g. the eruption of Mount Vesuvius in year 79 or the eruption of Krakatoa in year 1883, but it is also possible to observe waves produced by failure of the volcanic edifice. The latter case is usually modelled in the same way as landslide events by studying the interaction of the moving body with the water. For compact material, many features can be reproduced using a *solid-block model*, in which the deformation of the sliding body is ignored, as done by Tinti & Bortolucci (2000). This is not usually possible for volcanic materials that are often inconsistent and rheological effect cannot be ignored (see Zengaffinen et al., 2020). Finally, the least common causes are meteorological effects and the impact of meteorites. Fig. 1.2 shows the relative frequency of the possible causes.

Tsunami Propagation. Once the sea surface is displaced, the waves start propagating. It should be pointed out that separating generation and propagation is rigorously possible only in the case of an instantaneous source. This is approximately the case for explosions and tectonic events. The fault rupture and the coseismic displacements usually take a few seconds, reaching higher speed than the propagation of water waves, thus the event can be treated as instantaneous with respect to the propagation² On the other hand, mass wasting phenomena undergo more complex dynamics and their time dependence has to be taken into account and the separation of the two phases can be applied only when studying far-field properties of the tsunami.

As an order of magnitude estimation, the wavelength of the tsunami can be compared to a characteristic length of the source, e.g. for a tectonic event we may use the surface projection of the along-dip extension of the fault. Given that tsunamis are generated by great earthquakes ($M_w \gtrsim 7.0$), the typical wave length is in the order of tens or hundreds of kilometers and for this reason modelling is usually based of the *shallow water approximation*³. In the linear approximation, it can be shown that waves travelling over slowly varying bottom have phase speed given by

$$c(\mathbf{x})^2 = \frac{g}{k} \tanh(k h(\mathbf{x}))$$

where g is the gravity acceleration, k is the wavenumber and $h(\mathbf{x})$ is the sea depth as a function of the horizontal position \mathbf{x} . For long waves, the formula reduces to $c(\mathbf{x})^2 = g h(\mathbf{x})$, losing the dependence on the wavenumber and the model shows no dispersion effect. In this approximation, the propagation speed corresponding to the mean ocean depth, i.e. $h \approx 3.6$ km, is approximately 190 m s^{-1} , or 720 km h^{-1} . In recent years, dispersion effects have been observed and models with higher order approximation have been attempted, as shown by Glimsdal et al. (2013). The numerical computation of tsunami propagation is today a common practice for the purposes of both studying

²The general consideration about seismic events used from here on can be found in any text about seismology, as Udías & Buforn (2018) or Shearer (2019).

³The mathematical formulation of this approximation will be discussed in detail in the next chapters

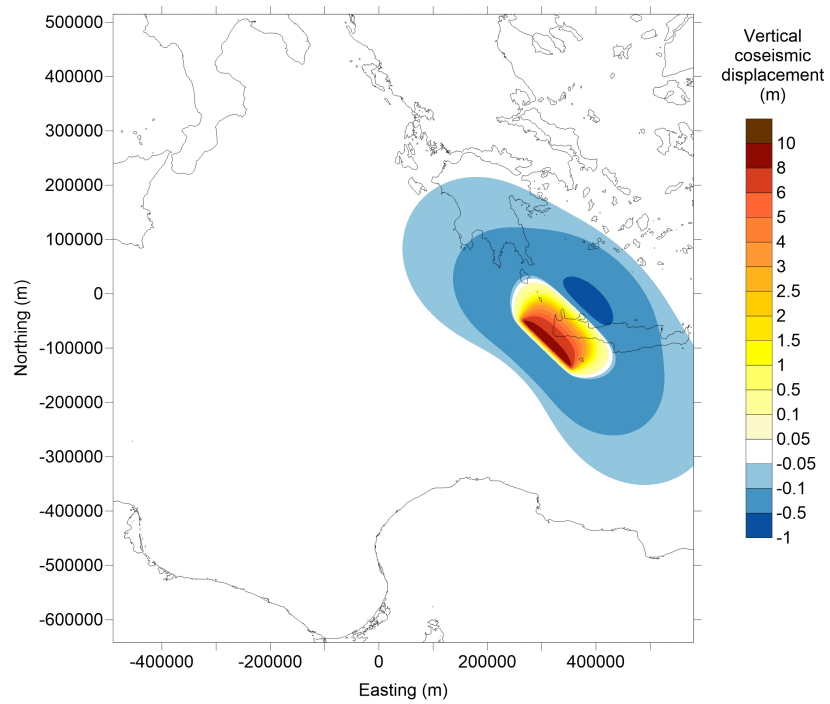


Figure 1.3: *Graphical representation of the initial water elevation generated by one of the faults proposed in the literature (Lorito et al. (2008)) as responsible for the 21 July 365 AD tsunamigenic earthquake along the western Hellenic trench. Image courtesy of the Tsunami Research Team at the Department of Physics and Astronomy, University of Bologna.*

possible future scenarios and simulating past events for which we have little to no data.

Fig. 1.3 and Fig. 1.4 show an example of a tsunami initial condition relative to a submarine earthquake and different snapshots of the propagation of the ensuing tsunami, respectively. The two Figures refer to a scenario similar to what may have happened on 21 July 365 AD, when an earthquake with estimated magnitude 8.3 – 8.5 ruptured a significant portion of the western Hellenic trench, with a large amount of slip released in proximity of the western coasts of Crete. The propagation of the tsunami has been simulated with the UBO-TSUFDF (Tinti & Tonini, 2013) shallow water numerical code.

Interaction with the coast. The *run-up problem* represents clearly the most impactful part of the process in terms of both damage of infrastructures and casualties. Despite this, it is still the least understood part of the tsunami process. First of all, the formulation is mathematically challenging:

- the interest is in the motion of the shoreline, so the problem involves a moving boundary;
- the inland evolution of the wave is governed by nonlinear equations.

As it will be discussed later, some results may be obtained also from the linearization of the problem.

Some aspects of the coast approaching wave may be derived from elementary physical considerations.

In addition to the theoretical aspects, there are a few more difficulties that are still to be precisely discussed and solved, as summarized by Levin (2016):

- firstly, we lack sufficiently detailed bathymetric profiles. In order to simulate the propagation of tsunami in the open sea, a resolution of a few kilometres is sufficient, but, due to the shortening of the wavelength, the resolution needed for precise run-up calculation should be much finer (up to few tens of meters or a few meters).

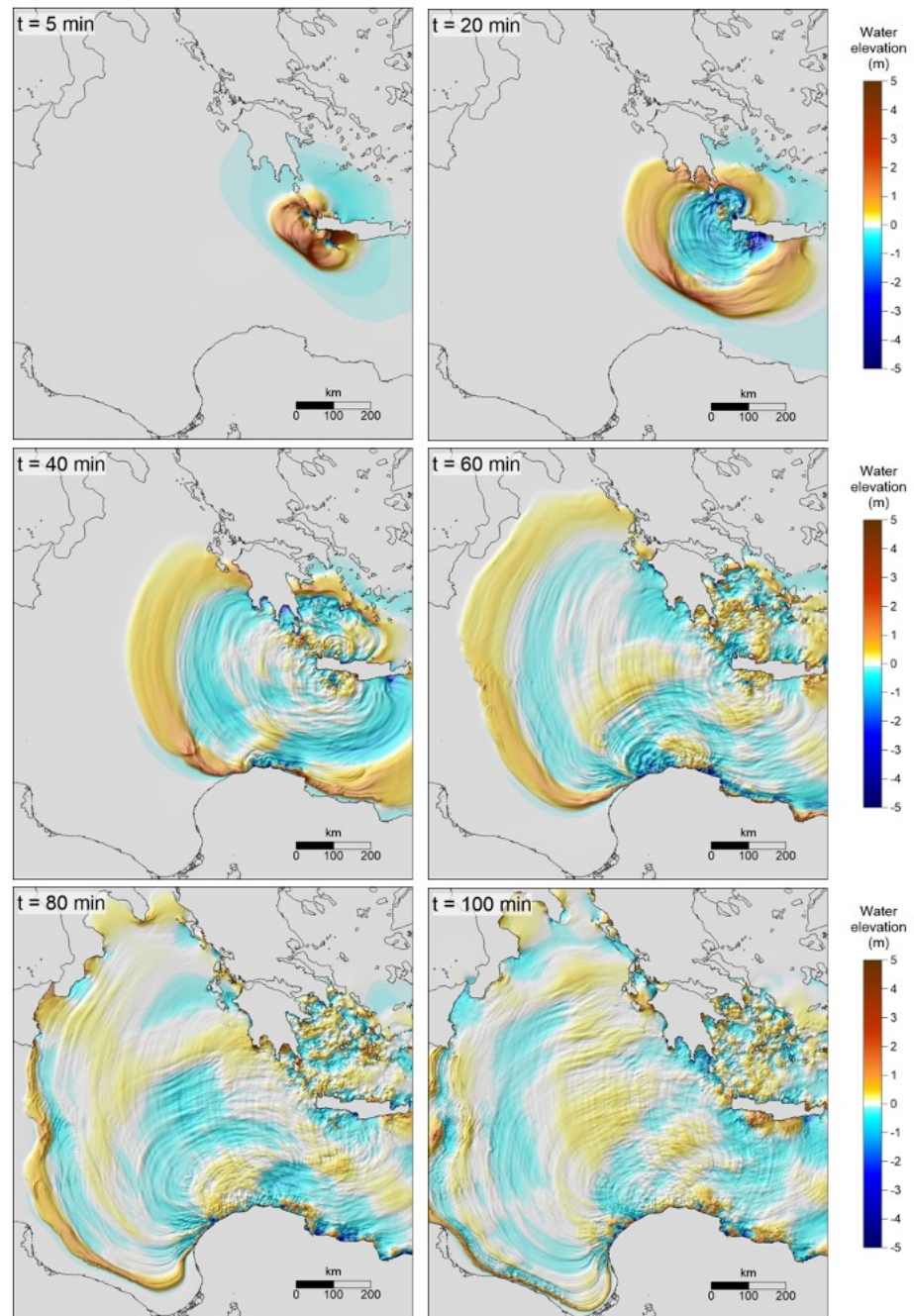


Figure 1.4: *Snapshots of the propagation of the tsunami with initial elevation from Fig. 1.3, simulated using the UBO-TSUFD model (Tinti & Tonini (2013)). Courtesy of the Tsunami Research Group at the University of Bologna.*

- secondly, there aren't many in situ measurements. Acquiring them has become a routine for recent events⁴, but for past events we need to rely on indirect measurements or historical testimonies.
- there is a coupling between wave motion and the geomorphology of the coastal environment, so we may expect strong tsunamis to be capable of changing the topography of the coast interacting with structures and/or vegetation.

1.2 A brief overview of the tsunami hazard and early warning topics

The main purpose of studying tsunami is obviously to prevent damage and casualties. However, the nature of the phenomenon, as previously described, makes the process of hazard assessment and early warning quite challenging. The main idea behind the brief excursus presented in this section is to highlight the importance of developing simple, yet rigorous and physically and mathematically well grounded, run-up models to be employed in general approaches for hazard and warning purposes.

As for other geophysical risks, two main approaches can be adopted for the hazard assessment, namely a deterministic or a probabilistic one. The former consists in the simulation of specific *scenarios* in order to predict the key features and metrics (e.g. wave height, propagation, inundation depth at coast, impact on buildings, etc...) of a tsunami caused by a specific source in a given region. The latter, similarly to the probabilistic seismic hazard analysis, uses a combination of a very large number of numerical scenarios, of analytical models or empirical relationships for the run-up process, and of observed statistical properties to establish the probability of an event with given characteristic to occur. Even with this simplified description, both approaches have glaring difficulties

⁴To have just some examples, see the works by Mori et al. (2011) for the 11 March 2011 Tohoku event, Fritz et al. (2011) for the 27 February 2010 Chile tsunami and Omira et al. (2019) for the 28 September 2018 Palu (Sulawesi) event.

that have to be addressed. First of all, the identification of tsunamigenic sources is far from trivial and it is usually addressed by using historical catalogues in combination with geological/geomorphological information, but even this adds some difficulties to the problem.

For example, let us consider the Italian Tsunami Catalogue (or ITC) by Tinti et al. (2004)⁵. Given that many entries in the catalogue are based on historical data, a *reliability* parameter is used to classify the events. It ranges between degree 0 (“very improbable tsunamis”) to 4 (“definite tsunamis”): out of the 72 currently listed events, 9 have a low reliability (either 0 or 1). Furthermore, the list is evidently incomplete: since 1600 an average of 16 tsunamis per century has been observed, while only 6 events are known in the period between the first documented event (caused by the Vesuvius eruption in 79 a.D.) and 1600. The geographical distributions of the historical events in this catalogue is shown in Fig. 1.5. The characterization of the *size* of the sources is also very heterogeneous:

- for volcanic eruptions, the explosivity index VEI is used, since it is commonly adopted to quantify the effect of historical events of this type;
- for tectonic sources, the *tsunami magnitude* is used as defined by Murty and Loomis (1980):

$$M = 2(\log E_P - 19) \quad \text{where } E_P = \frac{1}{2} \int \rho g h^2 ds$$

⁵In recent years various local catalogues have been merged into the unified Euro-Mediterranean Tsunami Catalogue (see Maramai et al. (2014)). Since we only want to exemplify some concepts, here we restrict ourselves to the last update of the Italian one available at http://roma2.rm.ingv.it/en/facilities/data_bases/27/catalogue_of_the_italian_tsunamis. General consideration may very well be used for other catalogues. At last, it is recalled that the number of events in a catalogue depends strongly on the interpretation of historical sources and the precise definition of tsunami employed. The Euro-Mediterranean Catalogue uses the Italian Catalogue as a primary source, so events reported in the two catalogues for the Italian area are also coincident, but for example the Global Historical Tsunami Catalogue (https://www.ngdc.noaa.gov/hazard/tsu_db.shtml) reports a higher number of events for the same region.

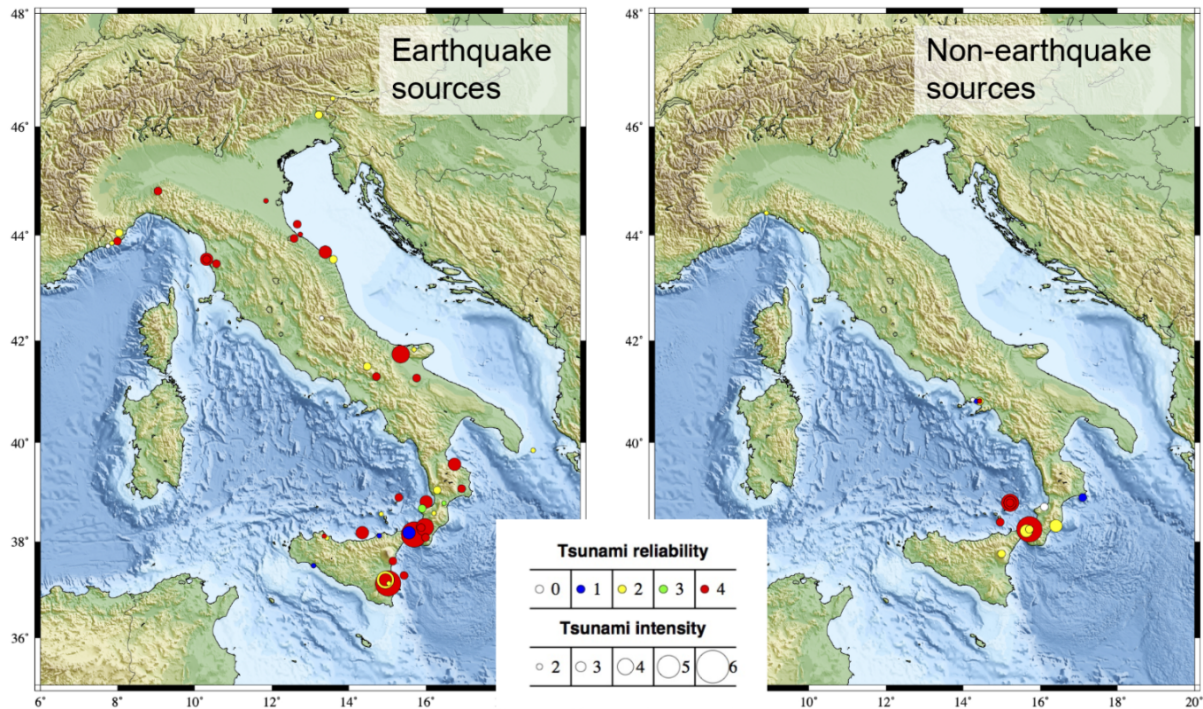


Figure 1.5: *Spatial distribution of historical tsunamis in Italy from the Italian Tsunami Catalogue (Tinti et. al. 2004, 2007).*

where E_P is the initial potential energy in erg, ρ is the density of water and h is the initial elevation. This formulation is suited for tectonic events since it relies on the instantaneousness of the source and it was developed to give the same value as the moment magnitude in the case of great earthquakes. However this formulation leads to big discrepancy in the case of low or medium size event, which is usually the case in the Italian region. The low applicability of this formula for historical data is evident by the fact that it is estimated only for 5 events on this catalogue.

- no general tool valid for all the source types has been found yet.

Another information reported is relative to the *tsunami intensity*, a scale that is used to describe the event based on the observed effects on the coast. The one used in ITC is a 6-degree scale developed by Sieberg and modified by Ambraseys (1962), varying from degree I, associated with tsunamis detected only by instruments, to degree VI,

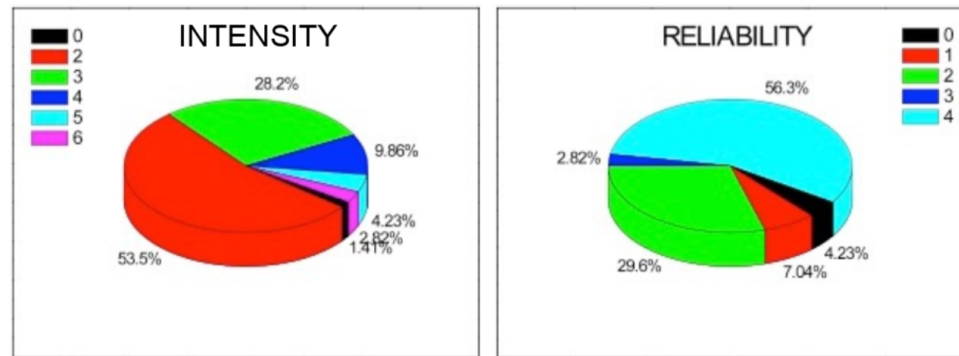


Figure 1.6: *Intensity and reliability distributions in the Italian Tsunami Catalogue (Tinti et. al. 2004, 2007).*

corresponding to total destruction of man-made structures and many casualties⁶. As an example, in Fig. 1.6 intensity and reliability distributions in the ITC are reported.

Once the sources have been identified, for the deterministic approach numerical simulations are carried out for specific scenarios. For this goal, various approximation of the Navier-Stokes equation are used over a discretized bathymetry, possibly with nested grids having finer resolution in coastal areas of particular interest. The individual scenarios are then used for the creation of *aggregated scenarios*: in each position of the impacted area, the selected value of a desired parameter is chosen as the most extreme among the ones calculated for a single source. This idea, that is part of the *worst credible case* approach, is detailed by Tinti & al. (2011) in the *Handbook of Tsunami Hazard and Damage Scenarios* and can be understood by an example: the aggregated maximum flooding area is obtained as the union of the maximum flooding area obtained in simulating each event. Finally, simulation are used to evaluate physical properties of

⁶It should be noted that other measures are found in the literature, defined mainly as logarithmic functions of the mean or maximum height registered by tide gauges. Although useful, they do not solve the problems briefly mentioned here: being measures of coastal height, they do not represent the source in the same sense of the magnitude. In addition to this, it has been argued by Papadopoulos and Imamura (2001) that an intensity scale should not be dependent of physical variables. Despite all of this, both the term *magnitude* and *intensity* are used for such functions in literature.

the wave that affect buildings, which are usually classified in standardized typologies for vulnerability and risk assessment.

The probabilistic approach, usually called *probabilistic tsunami hazard analysis* or PTHA, in analogy with the analogous method employed for seismic hazard, is quantified by means of statistical properties of the process. The generalities of the methods are given by Grezio et al. (2017). Given a finite set of possible tsunamigenic events, the idea is to compute the mean rate, i.e. the mean number per year, of events for which a certain *intensity parameter*⁷ reaches at least a given value. It is usually assumed that these event are *Poissonian* processes, i.e. they are treated as statistically independent.

In PTHA, a key information needed is the statistical behaviour of the source. In the case of tectonic events, a large number of studies have been carried out to establish their statistical properties, for which the most famous result is probably the Gutenberg-Richter relation

$$\log N(m) = a - bm$$

where m is the magnitude of the earthquake, $N(m)$ is the number of earthquakes with magnitude equal or greater than m and a and b are parameters usually obtained by regressions of catalogue data. It has been observed though that this loglinear relation breaks down for high magnitude events, for which there are typically not enough data to analyze. It has not been established yet what are the most appropriate statistical distributions for the other sources (landslides, volcanoes, ...).

Otherwise, empirical methods may be employed, which consist in fitting a probability model to the data provided by a catalogue or an instrument. Given the large variability of the tsunami effects even over small distances, empirical estimates may not be accurate, but they can be useful when it is difficult to account for every tsunami source. From what has been pointed out before, it is evident that statistical analysis must be performed carefully, since the completeness of the catalogue has to be taken into consideration.

⁷By intensity parameter we mean an arbitrary parameter we may use to quantify the tsunami which, despite the name, may not be the intensity discussed previously.

At last it may be important to highlight that in practice the probabilistic predictions and numerical modeling are combined. While in seismology it is common to use empirical relation, called *ground motion prediction equations* or GMPE, from empirical data, for tsunami numerical scenarios are used due to the scarcity of experimental measurements.

In recent years, particularly after the Sumatra earthquake and tsunami in 2004, there has been a global effort in the development of *tsunami early warning systems*, i.e. a real-time system that detects a possible tsunami so that the population in high risk areas can be alerted in time. A variety of instrumental measurements are used, for example:

- source characteristics can be extracted from a quick seismogram analysis, in the case of offshore earthquakes, or from volcanic observatories, in the case of violent eruptions;
- tide gauges and buoys offer data about wave propagation, allowing to detect and/or constrain possible tsunami waves;
- bottom pressure gauges can be used to detect the pressure perturbation that goes along with the wave, since the pressure variations induced by shallow water phenomena do not depend on the depth.

Once something is detected, warnings can be issued based on the use of simplified decision matrices (see for instance Tinti et al. (2012)) or by making use of more sophisticated, but computationally demanding approaches involving databases of pre-calculated scenarios. These scenarios usually do not compute precisely the inundation area, mostly because of the great computational effort needed; instead, simulations are carried out up to an arbitrary boundary (typically an isobath like 50 m or 20 m at a given distance from the coast). The run-up can then be predicted by applying suitable analytical models using waveforms computed numerically at the selected offshore isobath as initial conditions and propagating them over simplified linear, or piecewise linear, bathymetric profiles approximating the real nearshore bathymetry. Hence, the availability of suitable, reliable

and fast analytical run-up approaches, such as the one proposed in this thesis, can play a very important role.

1.3 Tsunami run-up from an analytical point of view

In the previous sections it has been highlighted that the run-up is one of the most important tsunami observables both to predict and to analyze. For this reason, a lot of effort has been put into its understanding from a theoretical point of view. The study of analytical run-up models has been started in the pioneering work by Carrier & Greenspan (1958). The problem is formulated in two dimensions (horizontal position and time) and it is assumed that the shallow water approximation holds. The authors then show that it is possible to find an analytical solution to the problem that is implicit in the horizontal position and time, from which the position and the velocity of the shoreline may be computed. At this point the inundated area can be found by finding the point of maximum height reached by the shoreline.

After the Carrier & Greenspan paper, many generalizations have been developed in order to have either easier computations or more realistic models. The original work assumed the presence of an initial water displacement with zero velocity as initial condition. This can be directly applied to the case of tectonic events, as proposed by Tinti & Tonini (2005): they assumed that the vertical coseismic displacement is transmitted identically and instantaneously to the water surface, and it is then parametrized in a form that allows for an analytical solution. Other initial conditions have also been studied, for example by Carrier, Wu & Yeh (2003) that added an initial velocity to the wave and expressed the solution in terms of a Green's function, so that a case with a general time dependent source can in principle be solved. This approach has been used by Özeren & Postacioglu (2012) to adapt the solution to a landslide generated tsunami.

Another important theme of research in the run-up topic is the relationship between linear and nonlinear solutions. The problem is highly nonlinear due to the form of the

shallow water equations and to the moving boundary, but a series of works, starting from the one by Synolakis (1987), has tried to understand if a linear approximation can be employed. As it will be shown in the next chapters, the linear approximation predicts the correct value of maximum and minimum run-up. This means that if we are interested in the inundation area, a linear approach may be sufficient with the advantages of lowering the computational time needed and allowing for easier generalizations. It has been used for example by Massel & Pelinovsky (2001) for dispersive and breaking waves. It is obvious that in the case in which the full history of the dynamics of the shoreline is needed, linear theory is not applicable.

At last, we note that some effort has been put into generalization to three dimensions, as attempted for example by Rybkin, Pelinovsky & Didenkulova (2014), who studied the run up in a channel with arbitrary cross section, a model suitable for long and narrow bays.

Chapter 2

Shallow Water Theory

In this chapter the *shallow water* approximation is exposed and discussed. The importance of the theory in geophysics can hardly be overestimated, due to the immense number of applications in meteorology, oceanography and solid earth physics. In particular the approach presented here is well suited for particular situations useful for some problems related to tsunami, since it is based on the assumption that the bottom movement and fluid surface disturbance have vertical and horizontal length respectively much smaller and much larger than the local fluid depth. For this reason, the equations we will get can be used to model waves produced by submarine landslides, offshore earthquakes or more general travelling long waves.

2.1 Basic Fluid Dynamics

The starting point in the mathematical description and modeling of tsunamis is represented by the equations of fluid dynamics in the hypothesis of inviscid fluid. The first is the momentum equation, also known as Euler equation, given by

$$\frac{\partial \mathbf{v}}{\partial t} + (\mathbf{v} \cdot \nabla) \mathbf{v} = \mathbf{g} - \frac{1}{\rho} \nabla p \quad (2.1)$$

where \mathbf{v} is the velocity field, \mathbf{g} is the gravitational acceleration and p is the pressure field. It describes the motion of a continuum in which the only surface interaction is given by pressure force and no viscous interaction is taken into consideration.

Another important equation is represented by the conservation of mass, whose general formulation is given by the continuity equation

$$\frac{\partial \rho}{\partial t} + \nabla \cdot (\rho \mathbf{v}) = 0 \quad (2.2)$$

However, this is not the form that will be used here. It can be shown that the speed of acoustic waves, or speed of sound, in a fluid is given by $c = \sqrt{K_S/\rho_0}$, where K_S is the isentropic incompressibility and ρ_0 is the density of the fluid at rest; for water we have $K_S \approx 2.2 \times 10^9$ Pa and $\rho_0 \approx 1000$ kg/m³, so that $c \approx 1480$ m/s. For fluid motion, the effects of compressibility, i.e. the variability of the density ρ , can be ignored in the case of isothermal situation in which particles and waves travels much slower than the speed of sound in that medium. As seen in the previous chapter, tsunami waves travels at approximately $v \approx 190$ m/s, so the ratio, usually called *Mach number*, is $M \equiv v/c \approx 0.13$ and compressibility effects are usually negligible if $M \lesssim 0.3$. Ignoring the variability of density, equation (2.2) reduce to

$$\nabla \cdot \mathbf{v} = 0 \quad (2.3)$$

The last assumption that is made is that the fluid is at rest before any excitation happens. In this configuration, the vorticity, defined as $\boldsymbol{\omega} = \nabla \times \mathbf{v}$, is zero, since the velocity is zero at every position. According the Kelvin theorem, the vorticity in an incompressible fluid in an inertial reference system remains constant with time. Thus, we obtain another equation for the problem given by

$$\nabla \times \mathbf{v} = 0 \quad (2.4)$$

At this point it is convenient to express the equations for the fluid using the components of the velocity field. Conventionally, the component of the fluid velocity vector along the Cartesian axes are indicated respectively by u, v, w and the equations (2.1), (2.3) and (2.4) can be written as

$$\frac{\partial u}{\partial x} + \frac{\partial v}{\partial y} + \frac{\partial w}{\partial z} = 0 \quad (2.5a)$$

$$\frac{\partial u}{\partial t} + u \frac{\partial u}{\partial x} + v \frac{\partial u}{\partial y} + w \frac{\partial u}{\partial z} = -\frac{1}{\rho} \frac{\partial p}{\partial x} \quad (2.5b)$$

$$\frac{\partial v}{\partial t} + u \frac{\partial v}{\partial x} + v \frac{\partial v}{\partial y} + w \frac{\partial v}{\partial z} = -\frac{1}{\rho} \frac{\partial p}{\partial y} \quad (2.5c)$$

$$\frac{\partial w}{\partial t} + u \frac{\partial w}{\partial x} + v \frac{\partial w}{\partial y} + w \frac{\partial w}{\partial z} = -\frac{1}{\rho} \frac{\partial p}{\partial z} - g \quad (2.5d)$$

$$\frac{\partial w}{\partial y} = \frac{\partial v}{\partial z}, \quad \frac{\partial u}{\partial z} = \frac{\partial w}{\partial x}, \quad \frac{\partial v}{\partial x} = \frac{\partial u}{\partial y} \quad (2.5e)$$

where the reference system is chosen so that the z -axis is directed upward and $\mathbf{g} = (0, 0, -g)$.

To explicitly solve fluid dynamics problems we now need to specify the boundary, which means we need to define the geometry and the initial condition of the problem. Let us call the surface displacement as $\xi(x, y, t)$. The presence of the free surface and the bottom imposes conditions on the velocity field. Firstly, it is assumed that the fluid does not detach nor penetrate the bottom and this is realized by imposing that the normal component of the velocity is given by the material derivative of the bottom surface. For later convenience, the bottom surface is expressed as the sum of two terms

- the first term is given by the static bottom bathymetry, described by the equation $z = -h(x, y)$;
- the second term represents the time-dependent component that excites the motion, that will be indicated as $h_s(x, y, t)$.

The condition will then be expressed by

$$u \frac{\partial h}{\partial x} + v \frac{\partial h}{\partial y} + w = \frac{\partial h_s}{\partial t} \quad \text{at } z = -h(x, y) + h_s(x, y, t) \quad (2.6)$$

Two other boundary conditions are imposed at the free surface $z = \xi(x, y, t)$:

- firstly we impose the external pressure, but since the interest is on waves caused by the moving bottom, the condition can be chosen as $p = 0$ at $z = \xi(x, y, t)$;
- secondly, the free surface is assumed to be a material surface, which means that the vertical component of the velocity field is equal to the time variation of the surface. It can be expressed as

$$\frac{\partial \xi}{\partial t} + u \frac{\partial \xi}{\partial x} + v \frac{\partial \xi}{\partial y} - w = 0 \quad \text{at } z = \xi(x, y, t) \quad (2.7)$$

At this point the problem is determined¹ and may be in principle resolved. Due to the non-linearity of the systems given by equations (2.5) through (2.7), it is not possible to find a general solution, but solutions for simplified situations can be determined.

2.2 Scaling analysis and perturbative expansion

Adimensionalising differential equations may help us understanding the relative importance of the various contributions and eventual approximations depend on the particular solution we may want to find; here we will follow Tinti & Bortolucci (2001) who studied the generation of waves by underwater slides. First of all, every physical quantity in the equations (2.5) through (2.7) is adimensionalised introducing scale parameters: the horizontal coordinates x and y are scaled with k , the vertical one z with D , time t with T , horizontal components of the velocity u and v with U , the vertical one w with W , the free surface elevation ξ with d , h with H , h_s with d_s and at last the ratio p/ρ is scaled with P . This means that, for example, the position is changed to $x' = x/k$ and analogous

¹In principle initial conditions have to be specified for the waveform and the speed. However, the shallow water approximation does not depend on this conditions, so for the moment they are omitted.

substitutions are made for every other variables. Equations (2.5) through (2.7) become

$$\frac{U}{k} \left(\frac{\partial u}{\partial x} + \frac{\partial v}{\partial y} \right) + \frac{W}{k} \frac{\partial w}{\partial z} = 0 \quad (2.8a)$$

$$\frac{U}{T} \frac{\partial u}{\partial t} + \frac{U^2}{k} \left(u \frac{\partial u}{\partial x} + v \frac{\partial u}{\partial y} \right) + \frac{UW}{k} w \frac{\partial u}{\partial z} = -\frac{P}{k} \frac{\partial p}{\partial x} \quad (2.8b)$$

$$\frac{U}{T} \frac{\partial v}{\partial t} + \frac{U^2}{k} \left(u \frac{\partial v}{\partial x} + v \frac{\partial v}{\partial y} \right) + \frac{UW}{k} w \frac{\partial v}{\partial z} = -\frac{P}{k} \frac{\partial p}{\partial y} \quad (2.8c)$$

$$\frac{W}{T} \frac{\partial w}{\partial t} + \frac{UW}{k} \left(u \frac{\partial w}{\partial x} + v \frac{\partial w}{\partial y} \right) + \frac{W^2}{k} w \frac{\partial w}{\partial z} = -\frac{1}{\rho} \frac{\partial p}{\partial z} - g \quad (2.8d)$$

$$\frac{W}{k} \frac{\partial w}{\partial y} = \frac{U}{k} \frac{\partial v}{\partial z} \quad \frac{W}{k} \frac{\partial w}{\partial x} = \frac{U}{k} \frac{\partial u}{\partial z} \quad \frac{U}{k} \frac{\partial v}{\partial x} = \frac{U}{k} \frac{\partial u}{\partial y} \quad (2.8e)$$

$$\frac{d}{T} \frac{\partial \xi}{\partial t} + \frac{dU}{k} \left(u \frac{\partial \xi}{\partial x} + v \frac{\partial \xi}{\partial y} \right) - Ww = 0 \quad \text{at } Dz = d\xi \quad (2.8f)$$

$$Pp = 0 \quad \text{at } Dz = d\xi \quad (2.8g)$$

$$\frac{UH}{k} \left(u \frac{\partial h}{\partial x} + v \frac{\partial h}{\partial y} \right) + Ww = \frac{d_s}{T} \frac{\partial h_s}{\partial t} \quad \text{at } Dz = -Hh + d_s h_s \quad (2.8h)$$

where the prime mark has been dropped for convenience.

Not all the scaling coefficients are independent. According to Buckingham's Π -theorem, if there are N parameters and M independent measurement units, then there exist $N - M$ independent dimensionless combinations of the parameters. In our case, $N = 9$ and $M = 2$ (the only fundamental quantities used are length and time), so there are 7 dimensionless groups that are needed in our system. Let us introduce the quantities $\{\Pi_i\}_{i=1}^7$ using k and $c = P^{1/2} = \sqrt{gD}$ as references for length and speed and define them as

$$\begin{aligned} \Pi_1 &= \frac{d}{k} & \Pi_2 &= \frac{d_s}{k} & \Pi_3 &= \frac{H}{k} & \Pi_4 &= \frac{D}{k} \\ \Pi_5 &= \frac{U}{c} & \Pi_6 &= \frac{W}{c} & \Pi_7 &= \frac{Tc}{k} \end{aligned} \quad (2.9)$$

so we obtain the equations

$$\frac{\Pi_4 \Pi_5}{\Pi_6} \left(\frac{\partial u}{\partial x} + \frac{\partial v}{\partial y} \right) + \frac{\partial w}{\partial z} = 0 \quad (2.10a)$$

$$\frac{\Pi_5}{\Pi_7} \frac{\partial u}{\partial t} + \Pi_5^2 \left(u \frac{\partial u}{\partial x} + v \frac{\partial u}{\partial y} \right) + \frac{\Pi_5 \Pi_6}{\Pi_7} w \frac{\partial u}{\partial z} + \frac{\partial p}{\partial x} = 0 \quad (2.10b)$$

$$\frac{\Pi_5}{\Pi_7} \frac{\partial v}{\partial t} + \Pi_5^2 \left(u \frac{\partial v}{\partial x} + v \frac{\partial v}{\partial y} \right) + \frac{\Pi_5 \Pi_6}{\Pi_7} w \frac{\partial v}{\partial z} + \frac{\partial p}{\partial y} = 0 \quad (2.10c)$$

$$\frac{\Pi_4 \Pi_6}{\Pi_7} \frac{\partial w}{\partial t} + \Pi_4 \Pi_5 \Pi_6 \left(u \frac{\partial w}{\partial x} + v \frac{\partial w}{\partial y} \right) + \Pi_6^2 w \frac{\partial w}{\partial z} + p_z + 1 = 0 \quad (2.10d)$$

$$\frac{\Pi_4 \Pi_6}{\Pi_5} \frac{\partial w}{\partial y} = \frac{\partial v}{\partial z} \quad \frac{\Pi_4 \Pi_6}{\Pi_5} \frac{\partial w}{\partial x} = \frac{\partial u}{\partial z} \quad \frac{\partial v}{\partial x} = \frac{\partial u}{\partial y} \quad (2.10e)$$

$$\frac{\Pi_1}{\Pi_6 \Pi_7} \frac{\partial \xi}{\partial t} + \frac{\Pi_1 \Pi_5}{\Pi_6} \left(u \frac{\partial \xi}{\partial x} + v \frac{\partial \xi}{\partial y} \right) - w = 0 \quad \text{at } z = \frac{\Pi_1}{\Pi_4} \xi \quad (2.10f)$$

$$p = 0 \quad \text{at } z = \frac{\Pi_1}{\Pi_4} \xi \quad (2.10g)$$

$$\frac{\Pi_4 \Pi_5}{\Pi_6} \left(u \frac{\partial h}{\partial x} + v \frac{\partial h}{\partial y} \right) + w = \frac{\Pi_2}{\Pi_6 \Pi_7} \frac{\partial h_s}{\partial t} \quad \text{at } z = -\frac{\Pi_3}{\Pi_4} h + \frac{\Pi_2}{\Pi_4} h_s \quad (2.10h)$$

Up to this point no approximations have been made and equations (2.10) are equivalent to the original system (2.5) through (2.7). To approximate the problem, we put

$$\Pi_1 = \Pi_2 = \Pi_5 = \delta \quad (2.11a)$$

$$\Pi_3 = \Pi_4 = \epsilon \quad (2.11b)$$

$$\Pi_6 = \epsilon \delta \quad (2.11c)$$

$$\Pi_7 = 1 \quad (2.11d)$$

and these definitions are essentially the physical assumptions of the problem. Two parameters have been defined, the *aspect ratio* $\delta = d/D$, i.e. the ratio between the thickness and the horizontal extension of the bottom perturbation, and the *expansion parameter* $\epsilon = D/k$ which expresses the ratio between the ocean depth and the horizontal scale over which we study the problem. From relations (2.11), some considerations about the orders of magnitude of the involved variables may be extracted, in particular:

- the perturbation thickness and the wave height have comparable magnitude (see (2.11a));
- the horizontal length of the perturbation is comparable to the local depth (see (2.11b));
- the vertical component of the velocity is smaller than the horizontal ones (see (2.11c));
- the time scale considered is the one related to the propagation of waves (see (2.11d)).

The system of equations (2.10) then becomes

$$\frac{\partial u}{\partial x} + \frac{\partial v}{\partial y} + \frac{\partial w}{\partial z} = 0 \quad (2.12a)$$

$$\delta \left[\frac{\partial u}{\partial t} + \delta \left(u \frac{\partial u}{\partial x} + v \frac{\partial u}{\partial y} + w \frac{\partial u}{\partial z} \right) \right] + \frac{\partial p}{\partial x} = 0 \quad (2.12b)$$

$$\delta \left[\frac{\partial v}{\partial t} + \delta \left(u \frac{\partial v}{\partial x} + v \frac{\partial v}{\partial y} + w \frac{\partial v}{\partial z} \right) \right] + \frac{\partial p}{\partial y} = 0 \quad (2.12c)$$

$$\delta \epsilon^2 \left[\frac{\partial w}{\partial t} + \delta \left(u \frac{\partial w}{\partial x} + v \frac{\partial w}{\partial y} + w \frac{\partial w}{\partial z} \right) \right] + \frac{\partial p}{\partial z} + 1 = 0 \quad (2.12d)$$

$$\epsilon^2 \frac{\partial w}{\partial y} = \frac{\partial v}{\partial z} \quad \frac{\partial u}{\partial z} = \epsilon^2 \frac{\partial w}{\partial x} \quad \frac{\partial v}{\partial x} = \frac{\partial u}{\partial y} \quad (2.12e)$$

$$\frac{\partial \xi}{\partial t} + \delta u \frac{\partial \xi}{\partial x} + \delta v \frac{\partial \xi}{\partial y} - w = 0 \quad \text{at } z = \delta \xi(x, y, t) \quad (2.12f)$$

$$p = 0 \quad \text{at } z = \delta \xi(x, y, t) \quad (2.12g)$$

$$u \frac{\partial h}{\partial x} + v \frac{\partial h}{\partial y} + w = \frac{\partial h_s}{\partial t} \quad \text{at } z = -h(x, y) + \delta h_s(x, y, t) \quad (2.12h)$$

2.3 The shallow water approximation

At this point, it can be assumed that ϵ and δ are small. This can be expressed by a perturbative expansion in ϵ : a generic function is then expressed as

$$f(x, y, z, t) = \sum_{k=0}^{\infty} \epsilon^k f^{(k)}(x, y, z, t) \quad (2.13)$$

By expressing every function in the problem in this way, approximate solutions may be obtained. In particular, the *shallow water approximation* results from the leading (zeroth) order approximation, which is equivalent to the limit $\epsilon \rightarrow 0$. Since we are not going to investigate higher order terms, the (0) is omitted from hereafter. The system of non-dimensional equations is thus

$$\frac{\partial u}{\partial x} + \frac{\partial v}{\partial y} + \frac{\partial w}{\partial z} = 0 \quad (2.14a)$$

$$\delta \left[\frac{\partial u}{\partial t} + \delta \left(u \frac{\partial u}{\partial x} + v \frac{\partial u}{\partial y} + w \frac{\partial u}{\partial z} \right) \right] + \frac{\partial p}{\partial x} = 0 \quad (2.14b)$$

$$\delta \left[\frac{\partial v}{\partial t} + \delta \left(u \frac{\partial v}{\partial x} + v \frac{\partial v}{\partial y} + w \frac{\partial v}{\partial z} \right) \right] + \frac{\partial p}{\partial y} = 0 \quad (2.14c)$$

$$\frac{\partial p}{\partial z} + 1 = 0 \quad (2.14d)$$

$$\frac{\partial v}{\partial z} = 0 \quad \frac{\partial u}{\partial z} = 0 \quad \frac{\partial v}{\partial x} = \frac{\partial u}{\partial y} \quad (2.14e)$$

$$\frac{\partial \xi}{\partial t} + \delta u \frac{\partial \xi}{\partial x} + \delta v \frac{\partial \xi}{\partial y} - w = 0 \quad \text{at } z = \delta \xi(x, y, t) \quad (2.14f)$$

$$p = 0 \quad \text{at } z = \delta \xi(x, y, t) \quad (2.14g)$$

$$u \frac{\partial h}{\partial x} + v \frac{\partial h}{\partial y} + w = \frac{\partial h_s}{\partial t} \quad \text{at } z = -h(x, y) + \delta h_s(x, y, t) \quad (2.14h)$$

From equation (2.14d) it can be seen that

$$p = -z + f(x, y, t)$$

and the value of the function $f(x, y, t)$ can be obtained by (2.14g) so that

$$p(x, y, z, t) = \delta \xi(x, y, t) - z \quad (2.15)$$

so in shallow water theory the vertical pressure gradient is given only by the hydrostatic contribution and the pressure field caused by the travelling wave is rigidly transmitted on the whole water column. For this reason, tsunami waves can be detected by instruments on the ocean bottom, as mentioned in the previous chapter.

An expression for the vertical velocity can be obtained from equation (2.14a)

$$w(x, y, z, t) = - \left[\frac{\partial u}{\partial x} + \frac{\partial v}{\partial y} \right] z + F(x, y, t) \quad \text{for } -h + \delta h_s < z < \delta \xi(x, y, t) \quad (2.16)$$

which shows that w changes linearly with depth. The function $F(x, y, t)$ is determined using (2.14f)

$$F(x, y, t) = \frac{\partial \xi}{\partial t} + \delta \frac{\partial}{\partial x} [u(x, y, t)\xi(x, y, t)] + \delta \frac{\partial}{\partial y} [v(x, y, t)\xi(x, y, t)] \quad (2.17)$$

and equation (2.14h) becomes

$$\frac{\partial \xi}{\partial t} + \frac{\partial}{\partial x} [u(h - \delta h_s + \delta \xi)] + \frac{\partial}{\partial y} [v(h - \delta h_s + \delta \xi)] = \frac{\partial h_s}{\partial t} \quad (2.18)$$

where none of the involved functions depend on the vertical coordinate.

Equations (2.14b) and (2.14c) thus can be written as

$$\frac{\partial u}{\partial t} + \delta u \frac{\partial u}{\partial x} + \delta v \frac{\partial u}{\partial y} + \frac{\partial \xi}{\partial x} = 0 \quad (2.19a)$$

$$\frac{\partial v}{\partial t} + \delta u \frac{\partial v}{\partial x} + \delta v \frac{\partial v}{\partial y} + \frac{\partial \xi}{\partial y} = 0 \quad (2.19b)$$

The last three equations form a closed system for the variables ξ, u, v , to be complemented with suitable conditions. It is interesting to observe that all the nonlinear terms are multiplied by δ . As specified before, the interest on submarine landslide and faulting events allows us to assume the aspect ratio δ to be small and if it is at least as small as ϵ the nonlinear terms can be omitted. The linear form of the shallow water equations will then be

$$\frac{\partial \xi}{\partial t} + \frac{\partial(uh)}{\partial x} + \frac{\partial(vh)}{\partial y} = \frac{\partial h_s}{\partial t} \quad (2.20a)$$

$$\frac{\partial u}{\partial t} + \frac{\partial \xi}{\partial x} = 0 \quad (2.20b)$$

$$\frac{\partial v}{\partial t} + \frac{\partial \xi}{\partial y} = 0 \quad (2.20c)$$

Once a problem has been solved for ξ, u, v the other relevant functions can be derived by

$$w = - \left(\frac{\partial u}{\partial x} + \frac{\partial v}{\partial y} \right) z + \frac{\partial \xi}{\partial t} \quad \text{for } -h < z < 0 \quad (2.21a)$$

$$p = -z \quad \text{for } -h < z < 0 \quad (2.21b)$$

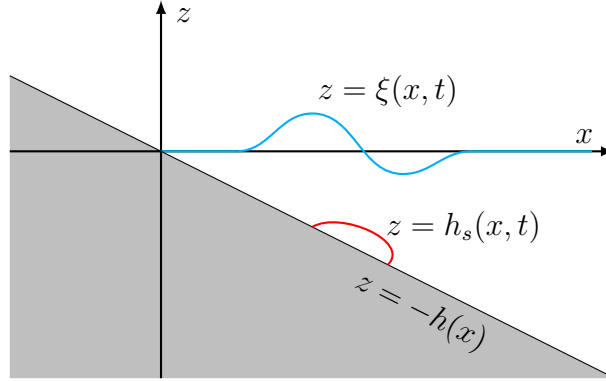


Figure 2.1: *Geometry of the problem over a uniformly sloping ocean bottom.*

The purpose of the rest of the work presented here is to develop (linear) analytical or semianalytical tools to study the run-up of tsunami waves. This is usually carried out in two dimension on the (x, z) -plane, so the equations to be solved will be

$$\frac{\partial \xi}{\partial t} + \frac{\partial(uh)}{\partial x} = \frac{\partial h_s}{\partial t} \quad (2.22a)$$

$$\frac{\partial u}{\partial t} + \frac{\partial \xi}{\partial x} = 0 \quad (2.22b)$$

$$w = -\frac{\partial u}{\partial x}z + \frac{\partial \xi}{\partial t} \quad \text{for } -h < z < 0 \quad (2.22c)$$

$$p = -z \quad \text{for } -h < z < 0 \quad (2.22d)$$

2.4 A General Solution for a Uniformly Sloping Ocean

At this point we adopt a specific ocean bottom profile. To study the evolution of waves in the coastal environment, a linear profile is the best suited for analytical development, so we put

$$h(x) = \alpha x \quad (2.23)$$

The first equations in (2.22) using the linear profile become

$$\frac{\partial \xi}{\partial t} + \alpha u + \alpha x \frac{\partial u}{\partial x} = \frac{\partial h_s}{\partial t} \quad (2.24a)$$

$$\frac{\partial u}{\partial t} + \frac{\partial \xi}{\partial x} = 0 \quad (2.24b)$$

Initial conditions are also needed. Given the main interest of this work, the initial waveform and horizontal velocity may be assumed to be zero

$$\xi(x, 0) = 0 \quad (2.25a)$$

$$u(x, 0) = 0 \quad (2.25b)$$

Deriving equations (2.24) respectively by t and x , they become

$$\begin{aligned} \frac{\partial^2 \xi}{\partial t^2} + \alpha \frac{\partial u}{\partial t} + \alpha x \frac{\partial^2 u}{\partial t \partial x} &= \frac{\partial^2 h_s}{\partial t^2} \\ \frac{\partial^2 u}{\partial t \partial x} + \frac{\partial^2 \xi}{\partial x^2} &= 0 \end{aligned}$$

and eliminating the u from the first, we obtain the following differential problem

$$\frac{\partial^2 \xi}{\partial t^2} - \alpha \frac{\partial}{\partial x} \left(x \frac{\partial \xi}{\partial x} \right) = \frac{\partial^2 h_s}{\partial t^2} \quad (2.26a)$$

$$\xi(x, 0) = 0 \quad (2.26b)$$

$$\frac{\partial \xi(x, 0)}{\partial t} = \frac{\partial h_s(x, 0)}{\partial t} \quad (2.26c)$$

where the second initial condition derives from evaluating (2.24b) at $t = 0$.

Integral transform approach. The following differential problem

$$\frac{\partial^2 \xi}{\partial t^2} - \alpha \frac{\partial}{\partial x} \left(x \frac{\partial \xi}{\partial x} \right) = f(x, t) \quad (2.27a)$$

$$\xi(x, 0) = 0 \quad (2.27b)$$

$$\frac{\partial \xi(x, 0)}{\partial t} = g(x) \quad (2.27c)$$

that closely resembles the set of equations (2.26a), can be solved by the use of integral transform techniques. Firstly, a variable change can be useful, in particular $s = \sqrt{x/\alpha}$ so that

$$\frac{\partial}{\partial x} = \frac{2}{\alpha s} \frac{\partial}{\partial s}$$

and equation (2.27a) becomes

$$\frac{\partial^2 \xi}{\partial t^2} - \frac{1}{s} \frac{\partial}{\partial s} \left(s \frac{\partial \xi}{\partial s} \right) = f \left(\frac{\alpha s^2}{4} \right) \quad (2.28)$$

The use of integral transforms has the purpose of converting a differential problem into an algebraic one; thus, the solution of the problem consists of a trivial calculation followed by an inversion, that can usually be carried out by tabulated inverse transforms². Here we will employ two types of transforms, the first one being the *Hankel transform*: for a function $f(s)$ it is defined as

$$\mathcal{H}_0[f] \equiv \bar{f}(p) = \int_0^\infty s J_0(ps) f(s) ds \quad (2.29)$$

where we introduced J_0 , the *Bessel function* of order 0. The general n -th order Bessel function is the solution of the differential equation

$$x^2 y'' + xy' + (x^2 - n^2) y = 0$$

and it can be shown that its Taylor series expansion can be written as

$$J_n(x) = \sum_{m=0}^{\infty} \frac{(-1)^m}{\Gamma(n+1+m)m!} \left(\frac{x}{2}\right)^{n+2m}$$

We recall the following property

$$\mathcal{H}_0 \left[\frac{1}{s} \frac{\partial}{\partial s} \left(s \frac{\partial f}{\partial s} \right) \right] = -p^2 \mathcal{H}_0[f] \quad (2.30)$$

This identity is particularly useful in the case of PDE with cylindrical symmetry, as is the case for (2.28).

The second integral transform needed is the *Laplace transform*, that for a function $g(t)$ is defined as³

$$\mathcal{L}[g] \equiv \tilde{g}(\tau) = \int_{0^-}^{\infty} e^{-t\tau} g(t) dt \quad (2.31)$$

²As a reference about integral transforms and their applications, the book by Davies (2002) is recommended.

³The limit over the lower boundary, i.e. the fact that the integral starts from 0^- instead of 0 is usually neglected, but it is important since it specifies the inclusion of the origin point, clearing the way distributions have to be manipulated. The following property about the Laplace transform of the n -th derivative presents terms calculated at 0^- and the initial condition for the derivative is thus $\frac{\partial \xi(x, 0^-)}{\partial t} = g(x)$ and the minus over the zero will be assumed from here on.

for which we recall the property

$$\mathcal{L} \left[\frac{d^n g}{dt^n} \right] = \tau^n \tilde{f}(\tau) - \sum_{k=0}^{n-1} \tau^k f^{(n-1-k)}(0^-) \quad (2.32)$$

To solve equation (2.28), we apply the Hankel transform to (2.28) with respect to the variable s , obtaining

$$\frac{\partial^2 \bar{\xi}}{\partial t^2} + p^2 \bar{\xi} = \frac{\partial f(\bar{p}, t)}{\partial t}$$

and then the Laplace transform with respect to the time t

$$\begin{aligned} \tau^2 \tilde{\xi} - \bar{g}(p, 0) + p^2 \tilde{\xi} &= \tilde{f}(p, \tau) \\ \tilde{\xi} &= \frac{\bar{g}(p, 0) + \tilde{f}(p, \tau)}{\tau^2 + p^2} \end{aligned}$$

To reverse the transforms, it is recalled that

$$\begin{aligned} \mathcal{L}^{-1} \left[\frac{1}{\tau^2 + p^2} \right] &= \sin pt \\ \mathcal{L}^{-1} [\tilde{f} \tilde{g}] &= (f * g)(t) \end{aligned}$$

so that we get⁴

$$\bar{\xi}(p, t) = \frac{\bar{g}(p) \sin pt}{p} + \frac{1}{p} \int_0^t \sin [p(t-t')] \tilde{f}(p, t') dt' \quad (2.33)$$

At this point take advantage of the fact that the inverse Hankel transform has the same form as the transform itself, which means

$$f(s) = \mathcal{H}_0^{-1} [\bar{f}] = \int_0^\infty p J_0(ps) \bar{f}(p) dp \quad (2.34)$$

so that the solution will be

$$\xi \left(\frac{\alpha s^2}{4}, t \right) = \int_0^\infty \bar{g}(p) \sin(pt) J_0(ps) dp + \int_0^\infty dp \int_{-\infty}^\infty dt' J_0(ps) \sin(p(t-t')) \tilde{f}(p, t') \quad (2.35)$$

⁴Technically, the convolution is defined over the interval $] -\infty; \infty[$, but the involved functions can be treated as *causal*, i.e. they are zero for $t < 0$. This may be assumed, since we are dealing with an initial value problem.

Now the transform \bar{g} and \bar{f} may be expressed using the definition (2.29) as

$$\xi\left(\frac{\alpha s^2}{4}, t\right) = \int_0^\infty dp J_0(ps) \int_0^\infty dr r J_0(rp) \left[g\left(\frac{\alpha r^2}{4}\right) \sin(pt) + \int_0^t dt' f\left(\frac{\alpha r^2}{4}, t'\right) \sin(p(t-t')) \right] \quad (2.36)$$

To solve the original problem (2.27a), we express ξ as a function of x and we introduce a new integration variable $q = \frac{\alpha r^2}{4}$ and $r dr = \frac{2}{\alpha} dq$, obtaining

$$\xi(x, t) = \frac{2}{\alpha} \int_0^\infty dp J_0\left(2p\sqrt{\frac{x}{\alpha}}\right) \int_0^\infty dq J_0\left(2p\sqrt{\frac{q}{\alpha}}\right) \left[g(q) \sin(pt) + \int_0^t dt' f(q, t') \sin(p(t-t')) \right] \quad (2.37)$$

This solution was first presented in an equivalent form by Tuck & Hwang (1972). They used it to investigate the waves generated by transient ground motion on a sloping beach, in order to analyse the near field features of the propagating waves. The approach assumed a displacement that decays exponentially starting from the origin with two possible time histories: a step function (in time) and transient motion that slowly approaches the maximum before an exponential decay. These particular cases were chosen in order to investigate the near and intermediate far-field behaviour of waves generated over a sloping beach, to compare the results with the nonlinear solutions computed numerically. In this work, it will be shown that a suitable parametrization of $h_s(x, t)$ allows for great simplifications of equation (2.37) when applied to run-up calculation, i.e., as it will be shown, in $x = 0$. It will also be shown that the assumptions needed for $h_s(x, t)$ are not much restrictive and applications to waves generated by near coast faults or underwater landslides will be given.

Chapter 3

Analytical Approaches to Run-Up Calculations

As pointed out before, the run-up problem plays a fundamental role in hazard assessment and early warning for tsunamis, since firstly it deals with the behaviour of the waves in the coastal area, and therefore the interaction with human settlements, and secondly it represents one of the tsunami observable easiest to measure, through in situ post-event surveys.

Some common assumptions are typical to nearly all the analytical studies. The preferred configuration is represented by a 2-dimensional setting over a uniformly, or piecewise uniformly, sloping beach, as in the case studied in the previous chapter. The physical model is almost always based on the shallow water approximation and wave breaking is ignored.

The problem is obviously nonlinear, but it will be argued that the linear approximation may be employed, since it is pretty much equivalent to the nonlinear one while being more easily generalizable.

3.1 Carrier & Greenspan Transformation

The pioneering work which is almost universally referred to as the foundation of the run-up analytical theory is the classic paper by Carrier & Greenspan (1958), in which the first analytical method for solving the problem has been presented. The starting point of the solution is given by the nonlinear shallow water equations

$$\frac{\partial u}{\partial t} + u \frac{\partial u}{\partial x} + g \frac{\partial \xi}{\partial x} = 0 \quad (3.1a)$$

$$\frac{\partial}{\partial x} [u(\xi + h)] + \frac{\partial \xi}{\partial t} = 0 \quad (3.1b)$$

where the notation and symbols are consistent with the previous chapters. These equations are simply the dimensional version respectively of (2.19) and (2.18) in the case of a 2-dimensional problem with $h_s = 0$.

To study the run-up problem, we introduce the sloping beach seen before, i.e. $h(x) = -\alpha x^1$. The solution method² consists in rewriting (3.1) in a form in which some characteristic variables act as independent variables and u , ξ , x and t are treated as unknown functions of this variable. The variables introduced by Carrier & Greenspan (1958) are defined through

$$\lambda = g\alpha t - u \quad (3.2a)$$

$$\sigma = 2\sqrt{g(\xi + \alpha x)} \quad (3.2b)$$

¹For the literature references, the lack of English language monograph on the run-up theme has to be pointed out, since it causes a great variety on the various formulations. For examples, Pelinovsky usually works with dimensional variables, as we are doing in this chapter, while Carrier & Greenspan adimensionalize. Furthermore, there are two definitions for the potential ψ that differ by a factor of 2. For this reason many results in this work are slightly different from the original ones, for the sake of consistency.

²Here we present a summary of the method following mainly Massel & Pelinovsky (2001). The original work shows how the variable substitution can be justified by the characteristic method typically used for hyperbolic problems.

To simplify the problem, a potential function $\psi(\sigma, \lambda)$ is defined by

$$u = -\frac{1}{\sigma} \frac{\partial \psi(\sigma, \lambda)}{\partial \sigma} \quad (3.3)$$

and the dependence on the new variables is

$$\xi = \frac{1}{2g} \left(\frac{\partial \psi}{\partial \lambda} - u^2 \right) \quad (3.4a)$$

$$x = -\frac{1}{2g\alpha} \left(\frac{\partial \psi}{\partial \lambda} - u^2 - \frac{\sigma^2}{2} \right) \quad (3.4b)$$

$$t = \frac{\lambda + u}{g\alpha} \quad (3.4c)$$

Using this transformation, sometimes called *hodograph transformation*, the equations (3.1) are reduced to a linear PDE for the potential

$$\frac{\partial^2 \psi(\sigma, \lambda)}{\partial \lambda^2} - \frac{\partial^2 \psi(\sigma, \lambda)}{\partial \sigma^2} - \frac{1}{\sigma} \frac{\partial \psi(\sigma, \lambda)}{\partial \sigma} = 0 \quad (3.5)$$

The solution of this equations requires two initial conditions. Following Carrier, Wu & Yeh (2003), let us consider the general case

$$\psi(\sigma, 0) = P(\sigma) \quad (3.6a)$$

$$\frac{\partial \psi(\sigma, 0)}{\partial \lambda} = F(\sigma) \quad (3.6b)$$

where the functions $P(\sigma)$ and $F(\sigma)$ can be expressed in terms of the velocity and surface elevation as

$$P(\sigma) = - \int_0^\sigma \sigma' u(\sigma', 0) d\sigma' \quad (3.7a)$$

$$F(\sigma) = 2g\xi(\sigma, 0) + u^2(\sigma, 0) \quad (3.7b)$$

respectively from equations (3.5) and (3.4a).

The problem can be solved using the Hankel transform in analogy with section 2.4; transforming equation (3.5) we get

$$\frac{\partial^2 \bar{\psi}}{\partial \lambda^2} + \rho^2 \bar{\psi} = 0 \quad (3.8)$$

which is an ODE in λ with solution

$$\bar{\psi}(\rho, \lambda) = \frac{1}{\rho} \bar{F}(\rho) \sin(\rho\lambda) + \bar{P}(\rho) \cos(\rho\lambda) \quad (3.9)$$

where ρ is the variable in the transform space and \bar{F} and \bar{P} are the transforms of the initial conditions (3.6).

By antitransforming, we get the solution in the (σ, λ) -space as

$$\psi(\sigma, \lambda) = \int_0^\infty F(b)G(b, \sigma, \lambda)db + \int_0^\infty P(b)\frac{\partial G(b, \sigma, \lambda)}{\partial \lambda}db \quad (3.10)$$

where the *Green function* is defined as

$$G(b, \sigma, \lambda) = b \int_0^\infty J_0(\rho\sigma) \sin(\rho\lambda) J_0(\rho b)d\rho \quad (3.11)$$

Despite having this analytical solution, there are some difficulties to overcome for its practical applications, in particular:

- it can be shown that the function defined in (3.11) can be expressed using elliptic integrals and it presents a singularity at $b = \lambda/2 - \sigma$, making the evaluation of the integrals in (3.10) tricky;
- the transformation from the (σ, λ) -space to the (x, t) -space is implicit, so the calculation of for a given time and/or position requires a numerical scheme, usually based on the Newton-Raphson algorithm (see Synolakis (1987));
- for the same reason, it is not obvious how to express the initial conditions as functions of σ . This is usually done by assuming the perturbation of the fluid surface is far from the origin, which is expressed by ignoring $O(u^2)$.

At last we note that expressing the solution (3.10) in terms of a Green function, we may be able to solve a more general form of equation (3.5) with a time-dependent, or λ -dependent, source term. This fact has been used by Özeren & Postacioglu (2012) to study the case of a submarine landslide. But to obtain the inhomogeneous form of (3.5),

they assumed the landslide height to be negligible w.r.t. the local ocean depth, which is also one of the hypothesis that leads to the linearization of the problem. This represents the first reason why a linear approach will be used here; in the next sections the same will be argued based on a formal analogy between a linear formulation of the problem and the nonlinear one obtained by the transformation (3.4).

3.2 Maximum run-up from nonlinear and linear solutions

The solution using the hodograph transformation gives implicitly the evolution of the full waveform. If we restrict our interest to the run-up, we have to extract from the solution the dynamics of the shoreline, that can be found as the intersection of the curves $z = \xi(x, t)$ and $z = -\alpha x$. By definition (3.2b), this means that the shoreline is described by the solution (3.10) by setting $\sigma = 0$ and therefore the run-up will be described by a *run-up function* $R(t) = \xi(\sigma = 0, \lambda)$, that describes the z -component of the moving shoreline. The x -component of the shoreline can be used as a measure of the inundated area and it can be calculated as $A(t) = -R(t)/\alpha$. In Fig. ?? the functions $R(t)$ and $A(t)$ are shown in relation with incident waveform. Despite the fact that the inundated area is one of the most important aspects of the tsunami run-up process, the function $R(t)$ is more frequently used, due to its invariance w.r.t. α for initial value problems and inhomogeneous problems as (2.27) when the source functions do not depend on α .

Let us now consider a linear formulation of the Carrier-Greenspan transformation. First of all, the *linear* shallow water equations will be

$$\frac{\partial u}{\partial t} + g \frac{\partial \xi}{\partial x} = 0 \quad (3.12a)$$

$$\frac{\partial \xi}{\partial t} + \frac{\partial hu}{\partial x} = 0 \quad (3.12b)$$

As before, we study the simple case where $h(x) = \alpha x$. The linear version of the trans-

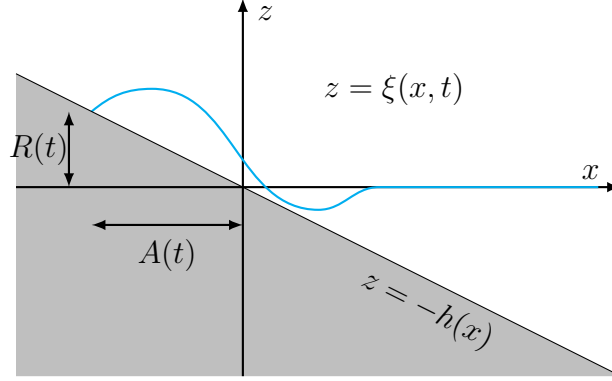


Figure 3.1: Representation of the waves approaching the coast. $R(t)$ is the run-up function and $A(t)$ is the inundation function.

formation (3.4) will be

$$u_0 = -\frac{1}{\sigma_0} \frac{\partial \psi_0}{\partial \sigma_0} \quad (3.13a)$$

$$\xi_0 = \frac{1}{2g} \frac{\partial \psi_0}{\partial \lambda_0} \quad (3.13b)$$

$$x = \frac{\sigma_0^2}{4g\alpha} \quad (3.13c)$$

$$t = \frac{\lambda_0}{g\alpha} \quad (3.13d)$$

where the subscript 0 is used to distinguish the functions from the ones in the nonlinear problem. By substituting (3.13) into (3.12) we obtain the equation

$$\frac{\partial^2 \psi_0(\sigma_0, \lambda_0)}{\partial \lambda_0^2} - \frac{\partial^2 \psi_0(\sigma_0, \lambda_0)}{\partial \sigma_0^2} - \frac{1}{\sigma_0} \frac{\partial \psi_0(\sigma_0, \lambda_0)}{\partial \sigma_0} = 0 \quad (3.14)$$

The similarities between the linear and the nonlinear formulations are evident. In fact, the potentials ψ and ψ_0 evolve according to analogous equations (respectively (3.5) and (3.14)) and they have the same asymptotes, since $\sigma \rightarrow \sigma_0$ and $\lambda \rightarrow \lambda_0$ far from the shoreline. The run-up from the linear theory can be calculated from the solution with $\sigma_0 = 0$, which means $x = 0$, and we obtain that $\xi(\sigma = 0, \lambda) = \xi_0(\sigma_0 = 0, \lambda_0)$. At last we note that for $u = 0$, we get $\lambda = \lambda_0$. From this an important conclusion is drawn: the

functions $\xi(x_s(t), t)$ and $\xi_0(0, t)$, where $x = x_s(t)$ is the kinematic equation of motion of the shoreline, have the same stationary point.

In conclusion, it has just been shown that the maximum run-up (and run-down) may be computed from a linear theory, giving the correct results. Nonetheless, the physics of the two solution is extremely different:

- the nonlinear solution gives as a result the complete dynamics of the shoreline, allowing for the computation of other functions, such as the shoreline velocity and the associated energy density flux;
- in the linear solution the boundary at $x = 0$ is fixed and the solution $\xi_0(0, t)$ describes the vertical motion of that point.

Despite the unphysical interpretation, the linear solution is more easily generalizable and the above discussion suggests its use whenever the main concern is the prediction of maximum run-up. This opens to many applications that are not directly treatable with the Carrier & Greenspan approach, such as in the case of wave breaking (see Pelinovsky & Massel (2001)), or that would require many simplifications and computational effort, such as with dynamical sources (see Özeren & Postacioglu (2012) for the use of the nonlinear approach for a landslide tsunami).

3.3 Linear solution for a fourier-series bottom excitation

In section 2.4, a general linear solution for the evolution of waves over a uniformly sloping beach has been developed and, as suggested in section 3.2, it can be used to evaluate the run-up of waves generated by ocean bottom time-dependent displacements.

If we define a *run-up function* as³ $R(t) = \xi(0, t)$, we get from equation (2.37) that

$$R(t) = \frac{2}{g\alpha} \int_0^\infty dp \int_0^\infty dq J_0 \left(2p \sqrt{\frac{q}{\alpha g}} \right) \left[g(q) \sin(pt) + \int_0^t dt' f(q, t') \sin(p(t-t')) \right] \quad (3.15)$$

since $J_0(0) = 1$ and we recall that

$$f(x, t) = \frac{\partial^2 h_s(x, t)}{\partial t^2} \quad (3.16a)$$

$$g(x) = \frac{\partial h_s(x, 0^-)}{\partial t} \quad (3.16b)$$

The factor g appears here because we want to use the equation in its dimensional form.

This linear solution can be useful if the following conditions are met:

- the computational time needed has to be low, so we might want to find some way to simplify the triple integration;
- it allows for a large number of general cases, not easily treatable with the a nonlinear approach.

Both conditions can be fulfilled by parametrizing the source function $h_s(x, t)$ as a *sine-Fourier transform* with time-variable spectrum

$$h_s(x, t) = \int_0^\infty A(\omega, t) \sin(\omega x) d\omega \quad (3.17)$$

and this can be obtained by assuming that h_s is zero in the origin, since an integral of this type is always an odd function. To simplify, another point of the x -domain is fixed: it is physically reasonable to assume that at a large distance L from the origin it will not be affected by the displacement h_s . In this way, the x -domain is limited to $[0; L]$ and the sine integral above becomes a series

$$h_s(x, t) = \sum_{n=1}^N A_n(t) \sin \frac{n\pi x}{L} \quad (3.18)$$

³From here on, only the linear formulation will be used, therefore the subscript 0 is dropped.

where N is assumed to be finite in view of its numerical evaluation. This parametrization allows for several possible general sources (both analytical and numerical) and it greatly simplifies the integrals in (3.15). To calculate the run-up solution we divide the solution into two terms:

$$R_1(t) = \frac{2}{\alpha g} \int_0^\infty dp \int_0^\infty dq J_0 \left(2p\sqrt{\frac{q}{\alpha g}} \right) g(q) \sin(pt) \quad (3.19)$$

$$R_2(t) = \frac{2}{\alpha g} \int_0^\infty dp \int_0^\infty dq J_0 \left(2p\sqrt{\frac{q}{\alpha g}} \right) \int_0^t dt' f(q, t') \sin(p(t-t')) \quad (3.20)$$

and we now work on $R_1(t)$. Obviously

$$g(x) = \sum_{n=1}^N \frac{\partial A_n(0^-)}{\partial t} \sin \frac{n\pi x}{L} \quad (3.21)$$

so we get

$$R_1(t) = \frac{2}{\alpha g} \sum_{n=1}^N \frac{\partial A_n(0^-)}{\partial t} \int_0^\infty dp \sin(pt) \int_0^\infty dq J_0 \left(2p\sqrt{\frac{q}{\alpha g}} \right) \sin \frac{n\pi x}{L} \quad (3.22)$$

We recall the notable integral

$$\int_0^\infty dx J_0(a\sqrt{x}) \sin(bx) = \frac{1}{b} \cos \frac{a^2}{4b} \quad (3.23)$$

where $a > 0, b > 0$, so that

$$R_1(t) = \frac{2L}{\alpha g \pi} \sum_{n=1}^N \frac{1}{n} \frac{\partial A_n(0^-)}{\partial t} \int_0^\infty dp \sin(pt) \cos \left(\frac{L}{\alpha g \pi n} p^2 \right) \quad (3.24)$$

Now we need another notable integral given by

$$\int_0^\infty dx \cos ax^2 \sin 2bx = \sqrt{\frac{\pi}{2a}} \left(\sin \frac{b^2}{a} C \left(\frac{b}{\sqrt{a}} \right) - \cos \frac{b^2}{a} S \left(\frac{b}{\sqrt{a}} \right) \right) \quad (3.25)$$

where $a > 0, b > 0$ and we introduced the *Fresnel integral functions*

$$S(x) = \frac{2}{\sqrt{2\pi}} \int_0^x dt \sin t^2 \quad (3.26a)$$

$$C(x) = \frac{2}{\sqrt{2\pi}} \int_0^x dt \cos t^2 \quad (3.26b)$$

so that finally

$$R_1(t) = \sqrt{\frac{2L}{\alpha g}} \sum_{n=1}^N \frac{1}{\sqrt{n}} \frac{\partial A_n(0)}{\partial t} \left[\sin\left(\frac{\alpha g \pi n}{4L} t^2\right) C\left(\sqrt{\frac{\alpha g \pi n}{4L}} t\right) - \cos\left(\frac{\alpha g \pi n}{4L} t^2\right) S\left(\sqrt{\frac{\alpha g \pi n}{4L}} t\right) \right] \quad (3.27)$$

For $R_2(t)$ we exchange the order of integration taking out the time integral and we repeat the same calculation done for $R_1(t)$. Let us introduce the notation

$$G(x) = \sin(x^2) C(x) - \cos(x^2) S(x) \quad (3.28)$$

and the total solution will be given by

$$R(t) = \sqrt{\frac{2L}{\alpha g}} \sum_{n=1}^N \frac{1}{\sqrt{n}} \left[\frac{\partial A_n(0^-)}{\partial t} G\left(\sqrt{\frac{\alpha g \pi n}{4L}} t\right) + \int_0^t dt' \frac{\partial^2 A_n(t')}{\partial t'^2} G\left(\sqrt{\frac{\alpha g \pi n}{4L}} (t - t')\right) \right] \quad (3.29)$$

This last formula consists in the sum of simple integrals, thus it is computationally less demanding than the general solution (2.37). Furthermore, no particular care is needed for the sum or the integrals, since N is finite and all the involved functions are smooth. In the end, the applicability of (3.29) depends on the applicability of (3.18): the use of a finite Fourier series to approximate a function is justified as long as the function does not present any jump discontinuity. In that case there would be an effect, called *Gibbs phenomenon*, for which large high frequency oscillations are observed in correspondence of the discontinuity points.

Finally, it is worth analyzing the influence of the ocean bottom slope on the solution. Let us assume that $h_s(x, t)$ does not depend on α and make the substitution $\alpha \mapsto \alpha k^2$. By changing the integration variable as $s = kt$ and scaling the partial derivatives as $\frac{\partial}{\partial t} = k \frac{\partial}{\partial s}$, the solution becomes

$$R(t) = \sqrt{\frac{2L}{\alpha g}} \sum_{n=1}^N \frac{1}{\sqrt{n}} \left[\frac{\partial A_n(0^-)}{\partial s} G\left(\sqrt{\frac{\alpha g \pi n}{4L}} s\right) + \int_0^{kt} ds \frac{\partial^2 A_n(s')}{\partial s'^2} G\left(\sqrt{\frac{\alpha g \pi n}{4L}} \left(\frac{t}{k} - s\right)\right) \right] \quad (3.30)$$

Equations (3.29) and (3.30) are equal up to a scaling of the time variable. This means that variations of the bottom slope change the arrival time of the wave, but leaves every other characteristic of the function $R(t)$ unchanged and in particular it does not influence its maximum and minimum values. It has to be pointed that we still need physically plausible values of α , so that the shallow water approximation holds.

Chapter 4

Applications to Tsunamigenic Earthquakes

Tsunamis are known to be originated by interaction of the solid earth with large bodies of water. In particular, as already recalled in chapter 1, the most frequent cause of tsunamis are earthquakes occurring offshore and capable of producing large vertical coseismic displacements, and landslides that either are triggered underwater or fall into water. They can all be thought as dynamical bottom displacements and, if the coseismic displacement field or the landslide height are small compared to the local water depth, the shallow water approximation, and therefore the solution presented in the previous chapter, is applicable.

4.1 Tectonic tsunamis

Many different theories have been developed in order to describe the process of tsunami generation. The common idea is that the coseismic displacement field caused by the earthquake on the ocean bottom causes a displacement of the free surface that then propagates in the ocean.

When the problem is treated analytically, some hypotheses are usually made:

- the fluid is considered incompressible;
- the rising time of deformation is small and often the process is treated as instantaneous;
- no coupling between the elastic bottom and the ocean is taken into account, other than during the deformation.

The validity of these assumptions has been discussed by Saito (2017).

Let us apply equation (3.29) to the case in which h_s is given by a coseismic field and let us factor it as

$$h_s(x, t) = u(x)M(t) \quad (4.1)$$

where $u(x)$ is the coseismic permanent displacements and $M(t)$ is a causal function of time that after a characteristic time τ is equal to one. If (3.18) is used, then we have

$$A_n(t) = \frac{2}{L} \int_0^L h_s(q, t) \sin\left(\frac{n\pi q}{L}\right) dq \quad (4.2)$$

that can be factored out as

$$A_n(t) = M(t) \left[\frac{2}{L} \int_0^L u(q) \sin\left(\frac{n\pi q}{L}\right) ddq \right] = M(t)U_n \quad (4.3)$$

where U_n are the coefficients of a sine Fourier series of $u(x)$, i.e. we have

$$u(x) = \sum_{n=1}^N U_n \sin\left(\frac{n\pi x}{L}\right) \quad (4.4)$$

As a time history function $M(t)$, a very simple one can be chosen

$$M(t) = \begin{cases} 0 & \text{for } t < 0 \\ t/\tau & \text{for } 0 \leq t \leq \tau \\ 1 & \text{for } t > \tau \end{cases} \quad (4.5)$$

where τ has the dimension of a time and plays the role of rising time of deformation.

To apply equation (3.29), we note that

$$\frac{\partial A_n(0^-)}{\partial t} = U_n \frac{dM(0^-)}{dt} = 0 \quad (4.6)$$

$$\frac{\partial^2 A_n(t)}{\partial t^2} = U_n \frac{d^2 M(t)}{dt^2} = \frac{1}{\tau} (\delta(t) - \delta(t - \tau)) \quad (4.7)$$

where $\delta(t)$ is the Dirac delta distribution. From here we get

$$R(t) = \sqrt{\frac{2L}{\alpha g}} \sum_{n=1}^N \frac{n^{-1/2} U_n}{\tau} \left[G \left(\sqrt{\frac{\alpha g \pi n}{4L}} t \right) - G \left(\sqrt{\frac{\alpha g \pi n}{4L}} (t - \tau) \right) \theta(t - \tau) \right] \quad (4.8)$$

where $\theta(t)$ is the Heaviside distribution. It is evident that in the limit $\tau \rightarrow 0$, i.e. when the displacement is assumed to be instantaneous, the formula becomes

$$R(t) = \sqrt{\frac{2L}{\alpha g}} \sum_{n=1}^N n^{-1/2} U_n \frac{d}{dt'} G \left(\sqrt{\frac{\alpha g \pi n}{4L}} t' \right)_{t'=t} \quad (4.9)$$

The function $u(x)$, that represent the coseismic displacement, is usually computed by means of the model developed by Okada (1985), which provides explicit formulas for displacement, deformation and stress caused by rectangular faults in an elastic, homogeneous and isotropic half-space. The fault is characterized by width W , length L , the depth of the upper edge D , the slip U and two angles, λ and δ that are respectively the direction of the slip on the plane, called *rake*, and the inclination of the fault w.r.t. to the surface, called *dip*. The geometry is shown in Fig. 4.1.

To apply the Okada model to the two dimensional case, we consider a fault whose trace is perpendicular to the x -axis and whose length L tends to infinity. It has been shown by Tinti & Tonini (2005) that in this case the vertical displacement is given by

$$\begin{aligned} u(x) &= \frac{U}{\pi} [U_s(x) \sin \delta + U_c(x) \cos \delta] \quad (4.10) \\ U_s(x) &= -\frac{(p-W)q}{(p-W)^2 + q^2} + \frac{pq}{p^2 + q^2} - \arctan \left(\frac{p}{q} \right) + \arctan \left(\frac{p-W}{q} \right) \\ U_c(x) &= -\frac{q^2}{p^2 + q^2} + \frac{q^2}{(p-W)^2 + q^2} \end{aligned}$$

where U is the slip, δ is the dip angle and $p = x \cos \delta + D \sin \delta + W$, $q = x \sin \delta - D \cos \delta$. Interestingly, this solution does not depend on the elastic parameters of the half-space

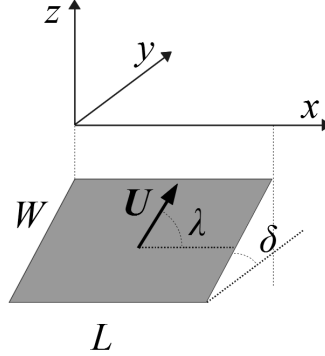


Figure 4.1: *Geometry of the Okada model. The fault is horizontal position is parallel to the x -axis. The parameter μ , ν are the Lamé parameters of the half-space, L is the length, W is the width, D is the depth of the upper edge, λ is the rake and δ is the dip.*

and it is therefore independent on the physical properties of the half-space. The sign is chosen so that when U is positive, the block on the right-hand side of the fault moves downward and the one on the left-hand side moves upward. To apply equation (4.9) to submarine faults, a translation is needed, meaning that an additional parameter is necessary, which is a position x_0 and the displacement will be $u(x - x_0)$.

One more point to make is that this model gives us the displacement at a horizontal plane, thus it is not strictly applicable to the case of a sloping bottom. However, only small value of the slope α will be considered and thus we assume that the bottom profile is given as the sum of a sloping term and the Okada displacement for a flat surface, as shown in Fig. 4.2. Since the coseismic displacement is at most of the order of a few metres, it is negligible w.r.t. the ocean depth, i.e. in the bathymetry $h(x) = -\alpha x + u(x)$ the coseismic displacement $u(x)$ smaller than αx . Therefore, in the following plots the linear term will be ignored and only the coseismic component will be shown.

The precision of the solutions depends on the properties of the Fourier series employed, that is based on the assumption that the position $x = 0$ and $x = L$ are fixed. The example given in Fig. 4.3 shows a vertical coseismic displacement field and its Fourier series approximation (equation (4.4) $N = 2000$). While in Fig. 4.3a the curves look very

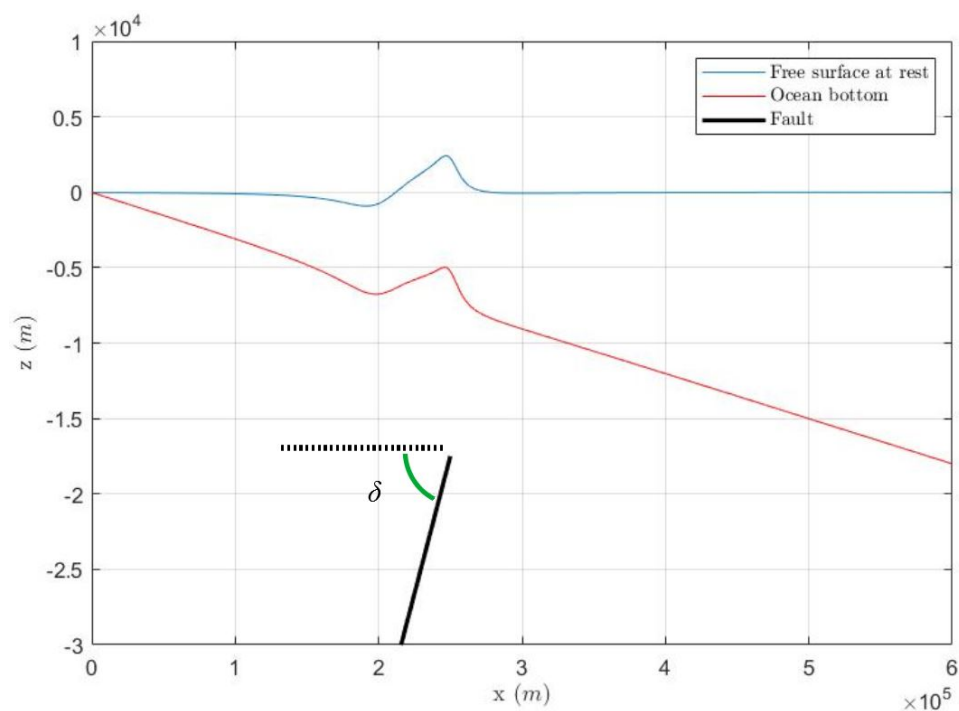
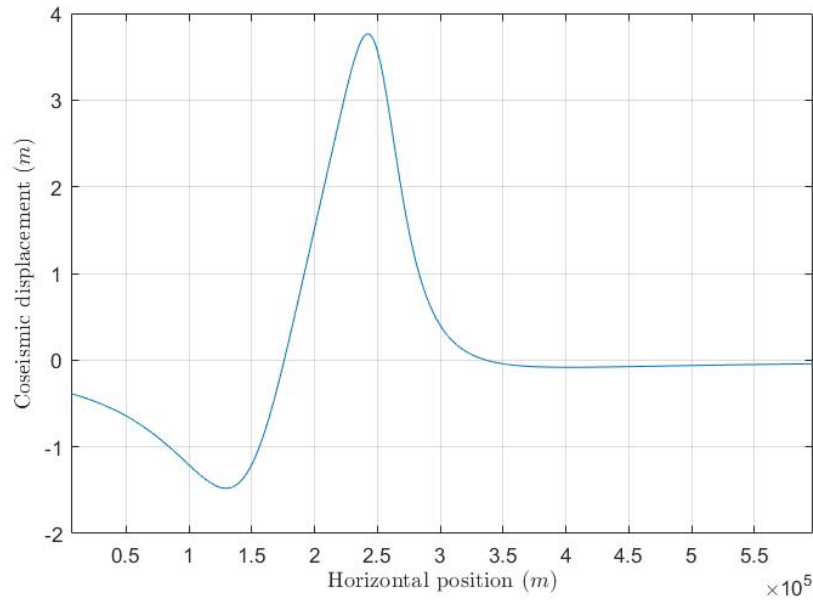
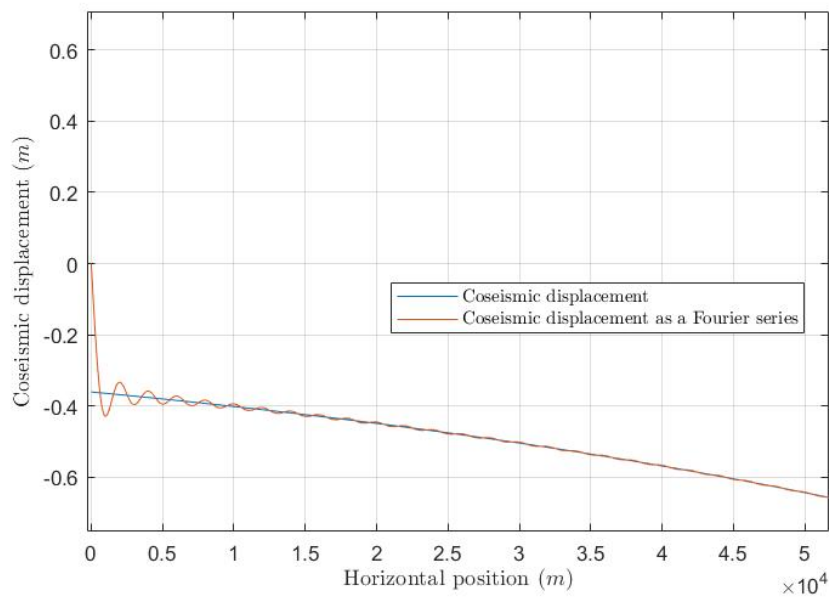


Figure 4.2: *Example of the displacement produced by a fault on the ocean bottom according to equations (4.10), transmitted instantaneously to the free surface. This representation is not in scale, since the order of magnitude of the maximum vertical displacement is around a few metres. The parameters are as follows: slip $U = 11.6$ m, fault width $W = 51.3$ km (as it will be explained later, these parameters correspond to an earthquake of $M_w \simeq 8.5$), depth $D = 10$ m, distance $x_0 = 250$ km, dip $\delta = 20^\circ$ and the coseismic displacement has been multiplied by 500 in order to be visible.*



(a)



(b)

Figure 4.3: An example of vertical displacement field obtained by means of the simplified Okada model given in (4.10) in (a). In (b) the behaviour at the origin is shown and its compared with the behaviour of the series representation. The oscillating behaviour due to the non zero deformation at the origin is evident. The parameters have been chosen to match the analogous example given by Liu & Sepúlveda (2016), as follows: $x_0 = 250$ km, $W = 100$ km, $D = 31.5$ km, $\delta = 20^\circ$, $U = 10.0$ m and $\alpha = 0.03$; the shoreline is in $x = 0$.

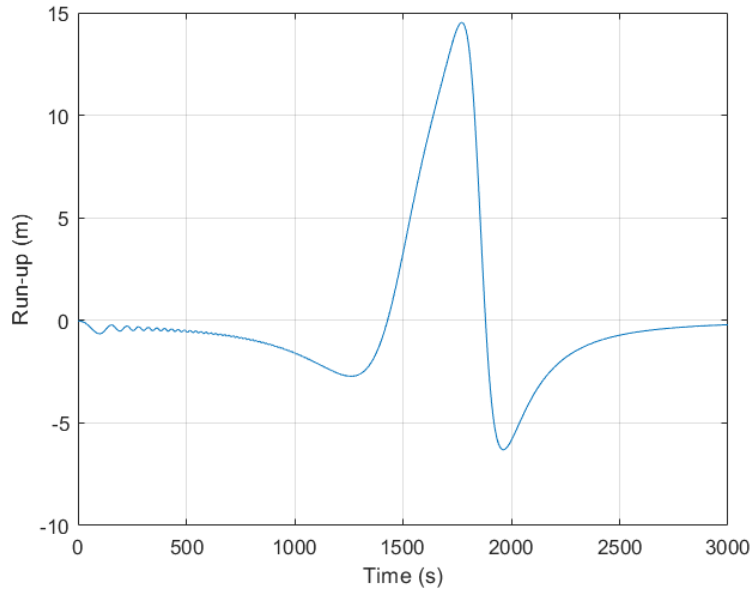


Figure 4.4: *Run-up function calculated using equation (4.9) for the model presented in Fig. 4.3.*

similar, it is evident from the particular in Fig. 4.3b that there is a discrepancy at the origin, caused by the fact that the $u(0) \simeq -0.36$ m. This generates spurious oscillations of the source term h_s near the origin, which then translates into the run-up solution, shown in Fig. 4.4. However, the solution is still valid for the purpose of this work: the oscillations in the run-up decay well before reaching any stationary point. Remembering that the linear theory predicts exactly only the stationary point of the run-up function, this artificial effect does not influence the results. The relevance of this problem is obviously proportional to the coseismic displacement at the origin, so the effect should be less evident for smaller and/or further located faults or for smaller earthquakes (i.e. a smaller value of the slip U). A crude way to take into account this effect may be using as an estimate for the maximum run-up the quantity $\max_{t \geq 0} R - u(-x_0)$, adjusting the measurements to the new reference frame by removing the new vertical position of the origin.

We also point out that the parameters chosen for the example in Fig. 4.4 are the same used by Liu & Sepúlveda (2016) and the predicted run-up function agree. This fact confirms the validity of the linear approximation, since the approach of Liu & Sepúlveda is based on the nonlinear equation and the hodograph transform (see chapter 3). Another important work we may want to compare our results with is Tinti & Tonini (2005). Despite being the main reference for the physical consideration of earthquake-induced tsunami, their examples are not testable with the present model. In fact their main concern is in fault under, or very near, the shoreline. This case would not give us reliable results, due to spurious oscillations mentioned before. The approach by Liu & Sepúlveda presents similar limitations.

A final consideration regards the way the coseismic displacement of the sea bottom is translated to the initial profile of the sea surface: clearly, this can have consequences on the final amplification of the wave at the coast. Following the previous discussion, it is assumed that the displacement $u(x)$ of the sea bottom is reached instantaneously and the compressibility effects are ignored. It has been shown by Kajiura (1963) that the waveform transmitted to the sea surface by a displacement over a flat ocean is given by

$$\xi(x, 0) = \frac{1}{\sqrt{2\pi}} \int_{-\infty}^{+\infty} dk e^{ikx} \frac{\tilde{u}(k)}{\cosh(kh)} \quad (4.11)$$

where

$$\tilde{u}(k) = \frac{1}{\sqrt{2\pi}} \int_{-\infty}^{+\infty} dx e^{-ikx} u(x) \quad (4.12)$$

is the Fourier transform of $u(x)$ and we observe that the ocean acts as a low-pass filter. Here, it is assumed that the shallow water approximation holds over the whole domain and this can formally be expressed in (4.11) by the limit $h \rightarrow 0$, thus getting

$$\xi(x, 0) \simeq u(x) \quad (4.13)$$

which means that the bottom displacement is transferred rigidly to the free surface.

4.2 Tsunami run-up dependence on the earthquake source

We now want to investigate the dependence of the maximum run-up on the source parameters of the earthquakes. To characterize earthquakes, two basic informations may be used:

- the *focal mechanism* describes the geometry of the source and it is equivalent to assign the angle between the surface and fault plane, called *dip*, the angle between the horizontal and the slip direction, called *rake*, and the angle between the fault trace and a chosen geographical direction (usually the North), called *strike*;
- the *magnitude* is the most used measure related to the *strength* of the earthquake.

We begin with the dependence on the focal mechanism. In the two dimensional case discussed here, only the *dip* angle is necessary to characterize the mechanisms: using the formulas (4.10), it is assumed that the *rake* is 90° , i.e. that the blocks move vertically one respect to the other (normal and reverse faults are represented by opposite signs of the slip U), and the *strike* is determined by the the fault trace being perpendicular to the x -axis.

Once determined the orientation of the fault, the other geometric information needed are the depth D , the width W , the length L and the slip U , from which the magnitude can be derived recalling the definition of *seismic moment*

$$M_0 = \mu LWU \quad (4.14)$$

where μ is the shear modulus of the half-space, which is related to the *moment magnitude*, defined by Hanks & Kanamori (1979)

$$M_w = \frac{2}{3} (\log_{10} M_0 - 9.1) \quad (4.15)$$

These definitions are not useful in our case, since the length L is assumed to be infinite, so another way to parametrize the problem is needed.

It is well known that the dimensions of faults are not independent from the magnitude and several scaling relations between magnitude and fault dimensions (ength, width, area) can be found in the literature. For example, Wells & Copperfield (1994)¹ found the following relations:

$$\log_{10}(|U|) = (0.69 \pm 0.08)M_w - (4.80 \pm 0.57) \quad (4.16a)$$

$$\log_{10}(W) = (0.32 \pm 0.02)M_w - (1.01 \pm 0.10) \quad (4.16b)$$

$$\log_{10}(L) = (0.59 \pm 0.02)M_w - (2.44 \pm 0.11) \quad (4.16c)$$

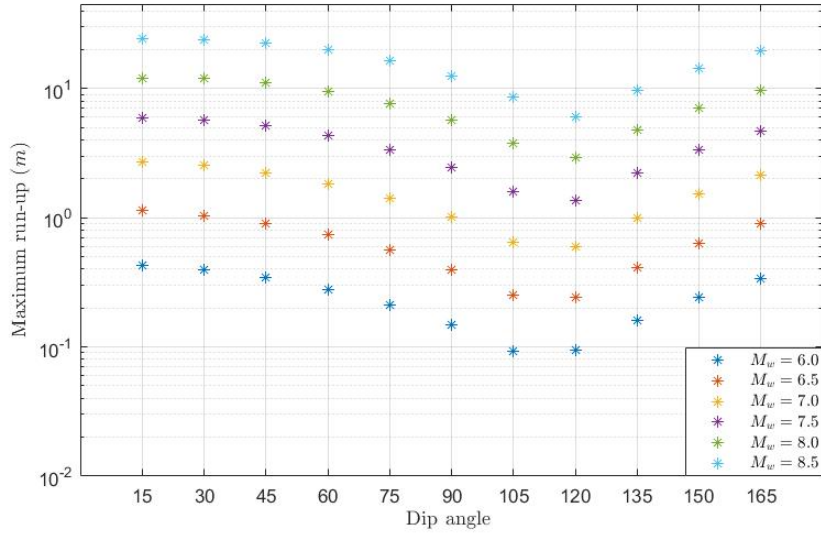
where W and L are in km, while U is in metre. Using equations (4.16), we can therefore use as free parameters the dip δ , the moment magnitude M_w , the depth D and the value of $\text{sgn}(U)$.

The variation of the maximum run-up for different dip angles and magnitudes is shown in figure 4.5. The first consideration that can be made is the power-law dependence on the magnitude for fixed dip, since the point along a vertical are more or less equidistant. This could be derived by theoretical considerations of the formulas used:

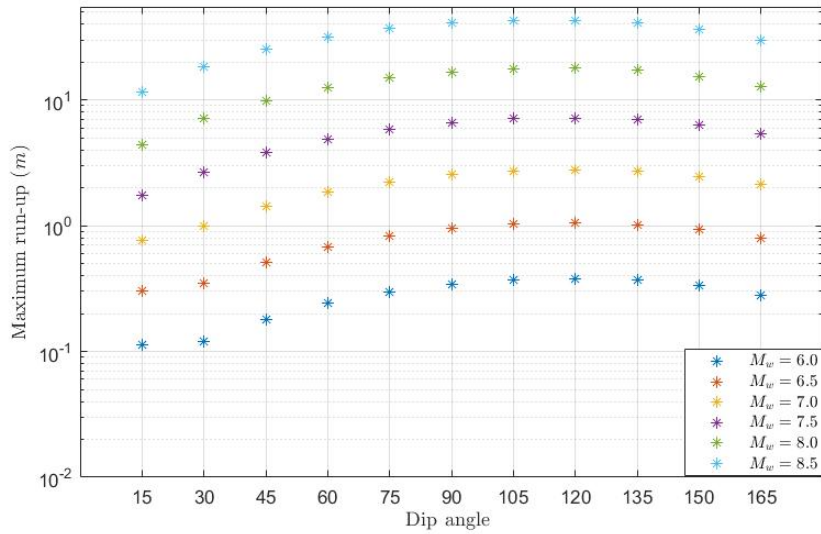
- the solution (3.29) is linear in the component of the discrete Fourier transform of the bottom displacement;
- the Fourier transforms are linear functional of the argument;
- the Okada model in (4.10) are linear with respect to the slip U ;
- equations (4.16) present a power-law dependence of U from the magnitude M_w .

It can also be noted that for a given magnitude, the dependence on the dip is strongly dependent on the sign of the slip. For positive slip, i.e. with the block facing the shoreline

¹Scaling properties of earthquakes represent an extremely vast subject and it is still debated to what extent they are applicable. Stirling & al. (2013) argue that usually little to no attention is given to the tectonic regime or to the quality and quantity of data. However, for the present purpose, the relations by Wells & Coppersmith are sufficient, since they are based on a global dataset and have been shown to be applicable to all focal mechanisms.



(a)



(b)

Figure 4.5: *Maximum run-up as a function of dip angles and magnitude. the distance has a fixed value $x_0 = 250$ km, as the fault depth $D = 10$ km, while fault width W and the absolute value of the slip U are computed from the magnitude using equations (4.16); the sign of U is positive for figure (a) and negative for (b). The correction for the coseismic displacement in the origin has been taken into account, although it does not exceed a few cm and it does not influence significantly the observed scaling properties.*

going downward, greater run-up is predicted when the fault forms small angles with the surface (with the maximum for 15° , while for negative slip, the maximum is reached around 120°). Anyway the cases of negative slip produce higher run-up: the maximum value in the former case is around 24.3 m, while for the latter is around 43.3m.

The few examples shown in Fig. 4.4 and 4.6 reveals a general property of this problem. If we consider the initial waveform as equal to the bottom displacement, it can be noticed that the second part of the wave, i.e. the half further from the shoreline is the most amplified in the process. In fact, the two examples in 4.6 show that the maximum run-up is achieved for dipoles travelling to the origin with leading depression.

Up to now the distance of the fault from the shoreline has been kept constant, but we can study how it influences the maximum run-up. Let us pick for example the most extreme case analyzed before, i.e. $M_w = 8.5$, $\delta = 120^\circ$ and negative slip. For a given seismic event, the dependence on the distance is not obvious, due to the nonlinear dependence on the position of the Okada model. However in Fig. 4.7, it is shown that the result of the linear calculation can be represented by a second degree polynomial fit; the maximum run-up for Fig. 4.7a are

$$R = (-1.11 \times 10^{-4}) x_0^2 + 0.107 x_0 + 7.31 \quad (4.17a)$$

$$R_c = (-7.86 \times 10^{-5}) x_0^2 + 0.0933 x_0 + 8.85 \quad (4.17b)$$

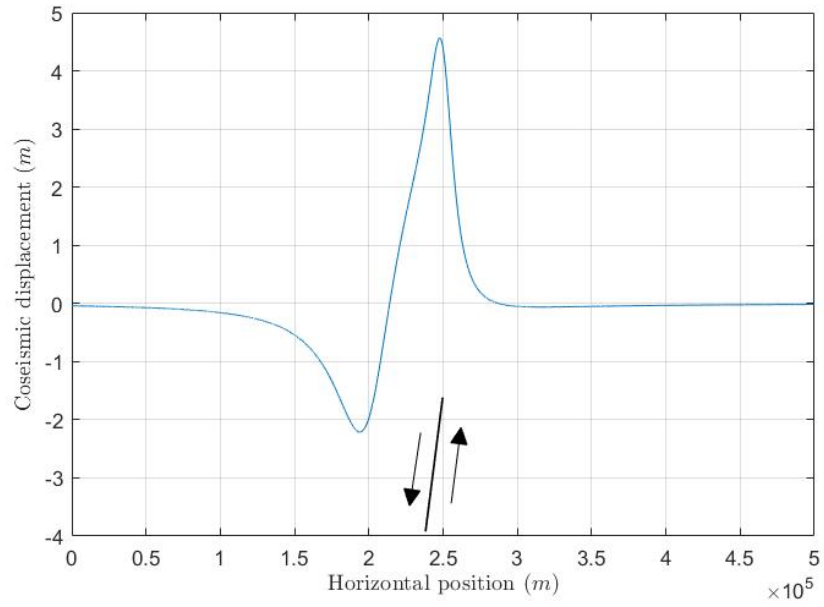
where R_c takes into account the coseismic correction at the origin, while R does not; x_0 is in km, R and R_c are in m. For Fig. 4.7b the analogous formulas are

$$R = (-1.74 \times 10^{-4}) x_0^2 + 0.177 x_0 + 14.8 \quad (4.18a)$$

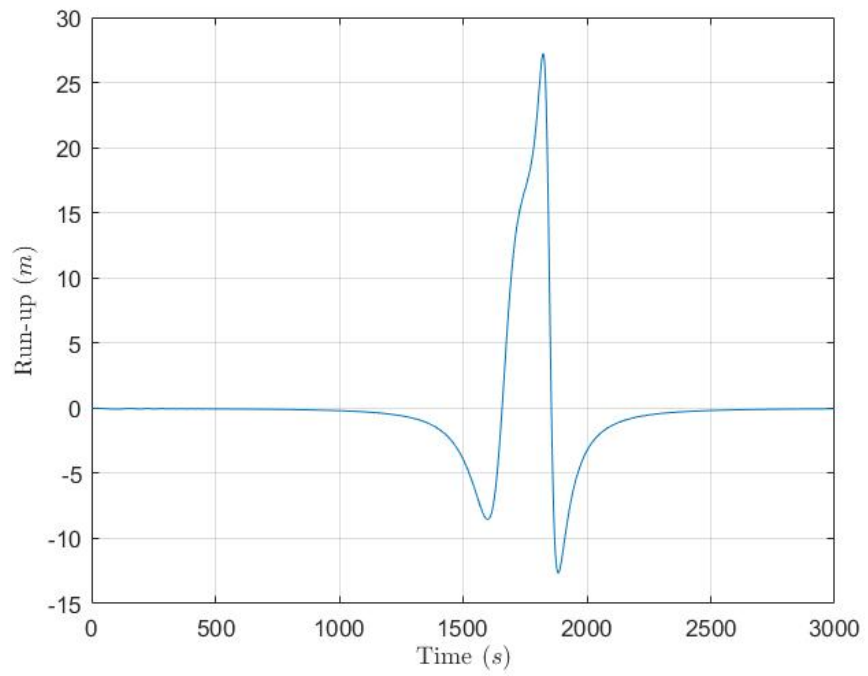
$$R_c = (-1.58 \times 10^{-4}) x_0^2 + 0.170 x_0 + 15.8 \quad (4.18b)$$

Polynomial fit such as the ones presented have obviously a limited range of validity, but from any practical point of view they can be useful, since outside these boundaries the model wouldn't work anyway. In fact, for smaller x_0 the influence of the *Gibbs phenomenon* is greater and the spurious oscillations do not decay before reaching the

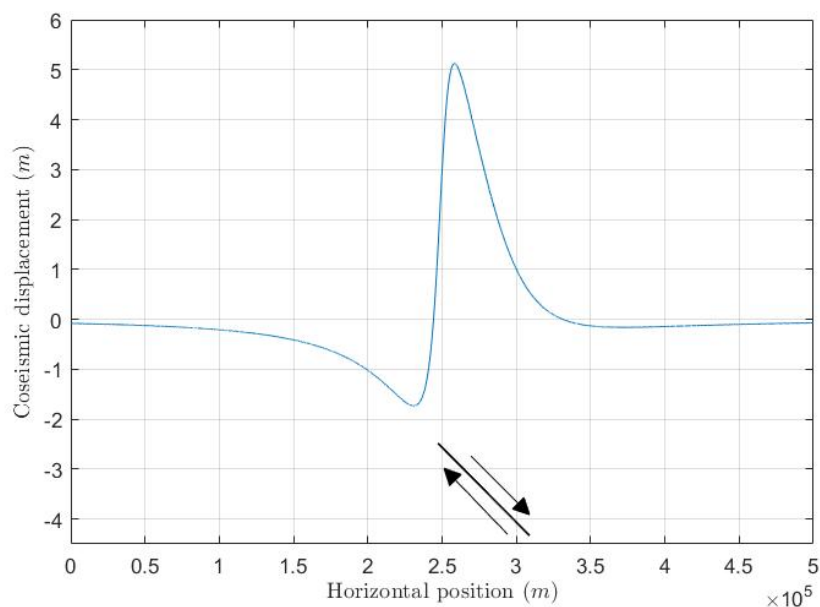
first stationary point. For bigger x_0 instead, calculations are not really needed: the last point in the plots corresponds to the value $x_0 = 250$ km, that for a slope $\alpha = 0.03$ corresponds to a depth $h(x_0) = 7.5$ km, which is more than twice the average ocean depth. Thus, such a model would not need extension for greater distances.



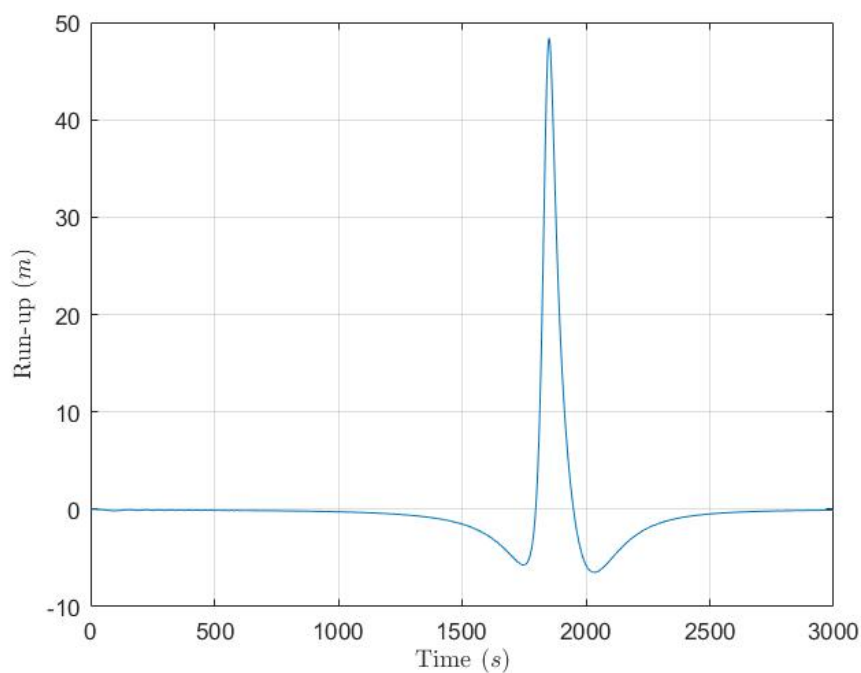
(a)



(b)

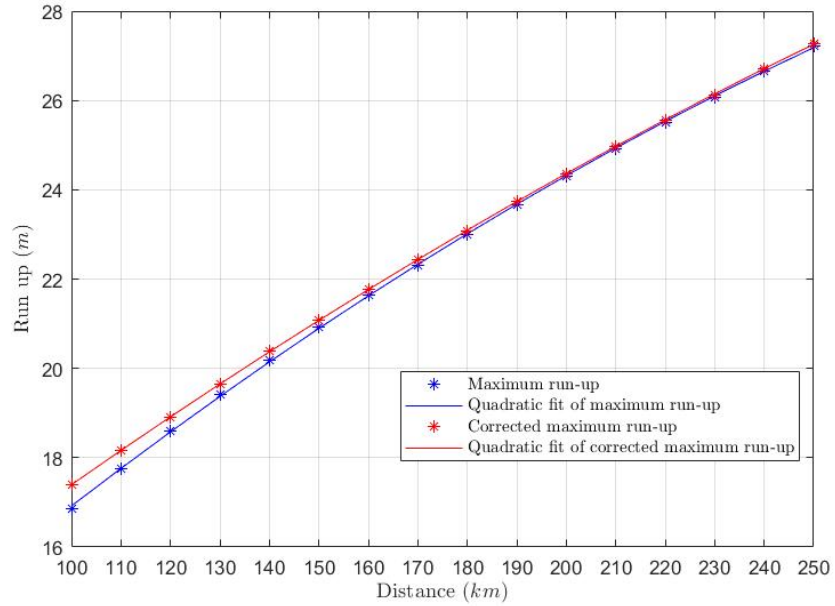


(c)

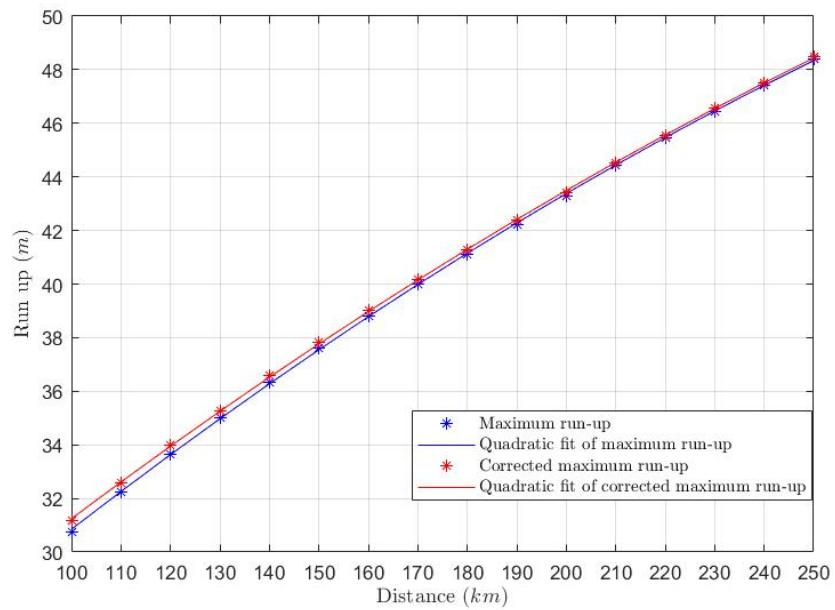


(d)

Figure 4.6: *Examples of bottom displacements calculated using equations (4.10) for positive slip and $\delta = 15^\circ$ (a) and for negative slip and $\delta = 120^\circ$ (c) and relative run-up calculations, respectively (b) and (d). The representation of the faults and the relative directions of motion for the two blocks is not in scale. All other parameters are the same as in figure 4.5.*



(a)



(b)

Figure 4.7: Maximum run-up as a function of the distance between the fault and the shoreline, both corrected and uncorrected for the coseismic displacement in the origin; a second degree polynomial fit is shown for all the cases. The parameters are chosen as follows: $D = 10$ km, $M_w = 8.5$, $\delta = 15^\circ$ and $\text{sgn}(U) = 1$ in (a), $D = 10$ km, $M_w = 8.5$, $\delta = 120^\circ$ and $\text{sgn}(U) = -1$ in (b).

Chapter 5

Applications to Tsunamigenic Landslides

5.1 Analytical landslide dynamics

A commonly used approximation for landslides used in analytical studies is the *solid block model*, which consists in considering the landslide as a non deformable body whose centre of mass moves according to a given kinematic law. This means that the shape of the moving mass does not change during the motion, so the ocean bottom displacement is expressed as the translation of the specified shape. Assuming that $h_s(x, 0) = p(x)$, i.e. the shape of the moving mass before moving is $p(x)$, the solid block assumption states that

$$h_s(x, t) = p(x - s(t)) \quad (5.1)$$

where $x = s(t)$ is the equation of motion of the center of mass of the body. Thus, to specify completely the motion of the landslide we need to find a suitable kinematic law $x = s(t)$.

Let us consider a rigid body of volume V , cross section S and characteristic length $L = V/S$ and density ρ_b . Following Pelinovsky & Poplavsky (1996), we consider the

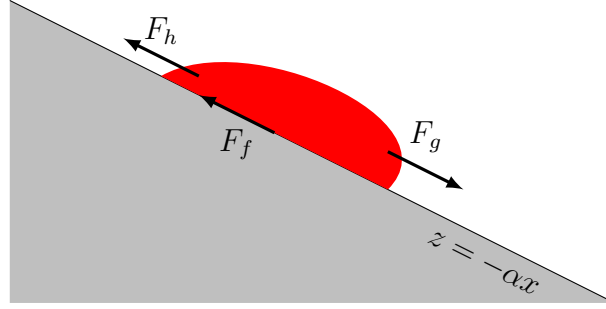


Figure 5.1: *Free body diagram of a landslide moving on an inclined plane subject to gravity (and buoyancy) F_g , a bottom sliding friction F_f and a hydraulic resistance F_h .*

following contributions:

- gravity and hydrostatic buoyancy given by

$$F_g = (\rho_b - \rho_w)gV \frac{\alpha}{\sqrt{1 + \alpha^2}}$$

where ρ_w is the density of water;

- a sliding friction given by the Coulomb law

$$F_f = (\rho_b - \rho_w)gV \mu \frac{1}{\sqrt{1 + \alpha^2}}$$

where μ is the sliding friction coefficient, assumed to be uniform;

- hydraulic resistance in the form

$$F_h = \frac{1}{2}\rho_w C_D S u^2$$

where C_D is the drag coefficient and u is the velocity of the body.

The equation of motion can be written in the form

$$\rho_b V \frac{du}{dt} = (\rho_b - \rho_w)gV \frac{\alpha - \mu}{\sqrt{1 + \alpha^2}} \quad (5.2)$$

where $u(t)$ is the velocity of the block. If we assume that the initial velocity is zero, we can make some important considerations. The initial acceleration a_0 can be found by imposing $u(t=0) = 0$:

$$a_0 = \frac{\rho_b - \rho_w}{\rho_b} g \frac{\alpha - \mu}{\sqrt{1 + \alpha^2}} \quad (5.3)$$

Furthermore, imposing $\frac{du}{dt} = 0$, we find an algebraic equation for the velocity once the acceleration is zero, i.e. the *terminal velocity*:

$$u_t = \sqrt{\frac{2gL}{C_D} \frac{\rho_b - \rho_w}{\rho_w} \frac{\alpha - \mu}{\sqrt{1 + \alpha^2}}} \quad (5.4)$$

and thus the equation of motion will be

$$\frac{du}{dt} = a_0 \left(1 - \frac{u^2}{u_t^2} \right) \quad (5.5)$$

whose solution is

$$u(t) = u_t \tanh \left(\frac{a_0}{u_t} t \right) \quad (5.6)$$

From Fig. 5.2, it can be seen that the parameters determine also how much time is needed to reach the terminal velocity and in particular the terminal velocity is reached faster for larger values of a_0/u_t . At this point, the kinematic law of motion needed in equation (5.1) can be expressed as

$$s(t) = \int_0^t u(t') dt' = \frac{u_t^2}{a_0} \ln \left(\cosh \left(\frac{a_0}{u_t} t \right) \right) \quad (5.7)$$

It should be pointed out that many other factors may influence the motion of the sliding mass, such as the added mass effect, lubrication effect on the bottom surface or the Basset force; a rich treatment of the possible terms we might add to equation (5.2) can be found in Watts (1997). Hereinafter, we make use of the model (5.7). In fact, if reasonable values for the initial acceleration and terminal speed are available, no other parameter is needed and the model is entirely kinematic.

5.2 Gaussian-shaped Solid Block

To apply the solid block model the shape $p(x)$ must be specified. A simple but effective model is given by a Gaussian shape in the form:

$$p(x) = a \exp\left(-\frac{x^2}{2b^2}\right) \quad (5.8)$$

where a is the height of the landslide and b is a measure of the horizontal extension. It can be shown that 95% of the area of $p(x)$ is in the interval $[-2b, 2b]$ and we can therefore define the *aspect ratio* as

$$r = \frac{a}{4b} \quad (5.9)$$

to represent the ratio between the vertical and the horizontal extension of the landslide. Some examples are shown in Fig. 5.3. The source function for a landslide that starts from the position x_0 will then be $h_s(x, t) = p(x - x_0 - s(t))$

The advantages of this particular choice of $p(x)$ are:

- due to the rapid decrease away from the centre, the model presents a *localized* mass without the need of generalized functions, that may cause problems from a computational point of view;
- it has been used in literature, in particular by Renzi & Sammarco (2016) to analyze the hydrodynamics of the landslide-induced tsunamis and by Özeren & Postacioglu (2012) to solve the run-up problem.

The calculation of the run-up functions can be done by direct application of equation (3.29). In Fig. 5.4 the run-up functions for various aspect ratios are shown. First of all, it can be noted that all the curves show a dipolar behaviour with a leading depression, i.e. at the minimum is reached before the maximum. This fact could have been deduced from the nature of the model itself: the motion of a solid block can be simplified as a moving dipole (see Pelinovsky & Poplavsky (1996)), where the mass is removed and added respectively in two consecutive positions and, since the block moves away from

the shoreline, the depression will be on the left. It can also be noted that the maximum run-up is larger for landslides with a bigger horizontal extension, while the minimum is smaller.

Let us consider the variation of maximum run-up with the kinematic parameters of the problem, i.e. a_0 and u_t . As we can see from Fig. 5.5a, the dependence of the maximum run-up has no obvious dependence on the terminal velocity. From equation (5.7), we understand that there is a spatial scale, that we can define as

$$s_0 = \frac{u_t^2}{a_0} \quad (5.10)$$

which represents the order of magnitude of the distance travelled by the landslide before it reaches the terminal velocity. In Fig. (5.5b), it is shown how the maximum run-up varies with s_0 for different values of the initial acceleration and every curve follow the same qualitative trend: there is a rapid increase up to s_0 around a few hundreds, then it slowly decreases. To understand how this affects the problem, let us consider $u_t \in [10 \text{ m s}^{-1} : 30 \text{ m s}^{-1}]$ (values used by Tinti & Bortolucci (2000)). We obtain:

- for $a_0 = 0.5 \text{ m/s}^2$, $s_0 \in [200 \text{ m} : 1800 \text{ m}]$, so the maximum run-up slowly decays with the terminal velocity;
- for $a_0 = 8.0 \text{ m/s}^2$, $s_0 \in [12.5 \text{ m} : 112.5 \text{ m}]$ and from Fig. 5.5b we can see that it corresponds to a high increase of maximum run-up with the terminal velocity.

To end the section, we also point out that the order of magnitude of the maximum run-up and its dipolar form are compatible with the results presented by Özeren & Postacioglu (2012). However, the direct comparison is not rigorously possible: they use equations similar to (5.3) and (5.4) to parametrize the motion of the sliding mass, but not all the parameters employed in their work are specified. Nonetheless, the values of u_t and a_0 used in the previous example represent realistic values for the problem (again, see Tinti & Bortolucci (2000), Tinti et al. (2001)), so the agreement of the orders of magnitude and of the qualitative form of the run-up is still an encouraging result.

5.3 A Hint on landslides with time-dependent shape

There are many real cases in which the solid block model is not applicable, in particular when the landslide is made of incoherent material. To study the influence of possible deformations, we may use equation (3.29) with a source function $h_s(x, t)$ with a time-dependent shape. Here, we propose a simple model in the following form:

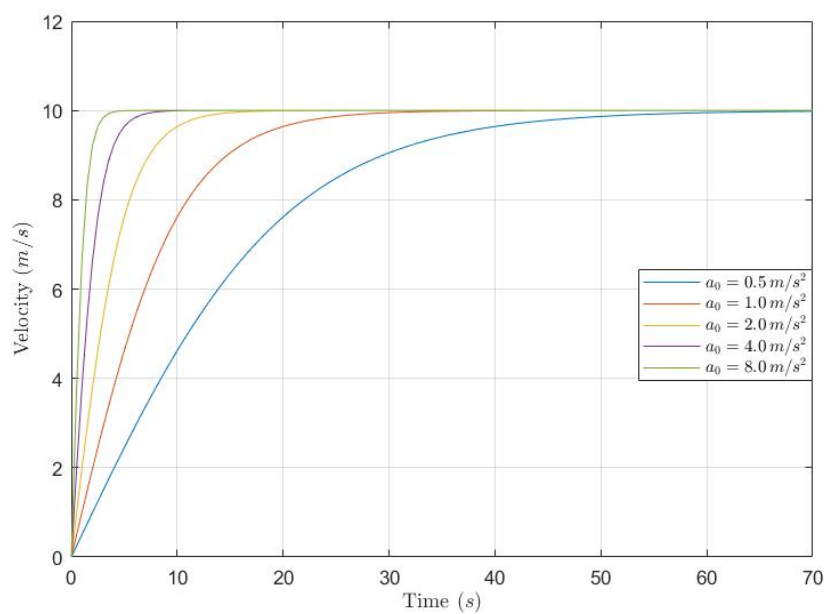
$$h_s(x, t) = \frac{a}{1 + ct} \exp\left(-\frac{1}{2} \left(\frac{x - x_0 - s(t)}{b(1 + ct)}\right)^2\right) \quad (5.11)$$

where the new parameter c has been introduced. To understand the meaning of this parameter, we note that $h_s(x, t)$ may be obtained from the solid block model with the following substitutions:

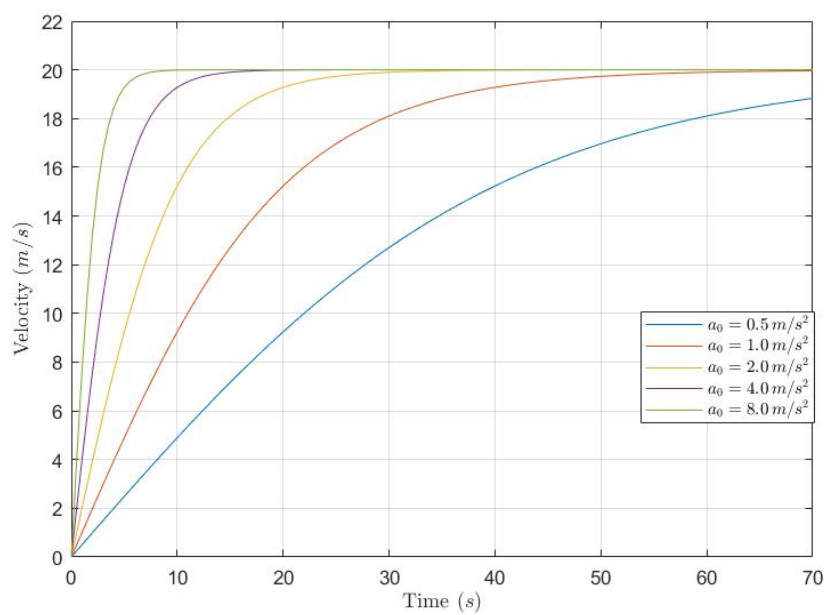
- $a \mapsto \frac{a}{1+ct}$, which means that the height of the landslides is halved after a time c^{-1} ;
- $b \mapsto b(1 + ct)$, which means that the landslide horizontal extension grows linearly with time.

So, c^{-1} represents a way to express how consolidated the body is. This situation might be used in the case of a granular mass wasting, since it tends to diffuse the concentration of mass away from the center. It should be noted that for $t \rightarrow \infty$ this model is not physical for $t \rightarrow \infty$, since it assumes that the moving mass diffuses until $h_s(x, t) = 0$ and, given that the domain is finite, the total mass is not conserved.

In Fig. 5.6, run-up functions for different values of c . For small values of c^{-1} , a strong increase of the maximum and minimum run-up occurs. If we consider as an example $c^{-1} = 20$ s, we have a moving body whose height is halved in 20 s and the solution is then equivalent to a rapid removal of material, i.e. a negative impulsive forcing. Since the model does not conserve the mass, low values of c^{-1} may not be physically meaningful for landslides. For larger values of c^{-1} , the run-up tends to the value predicted for a solid block and we can conclude that for the purpose of run-up calculation, the assuming a solid block condition is sufficient for the purpose.

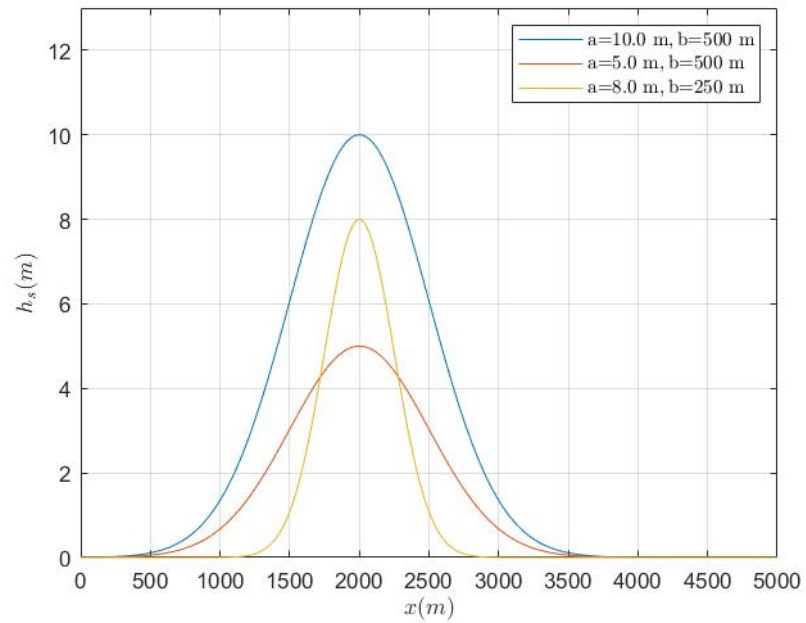


(a)

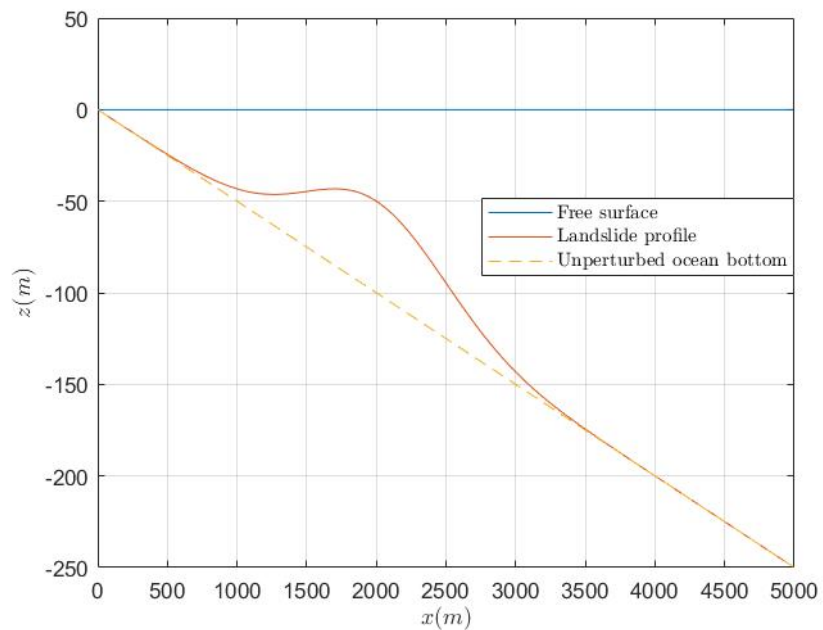


(b)

Figure 5.2: Velocity predicted by equation (5.6) varying the initial acceleration for fixed terminal velocity $v_t = 10 m/s$ and $v_t = 20 m/s$



(a)



(b)

Figure 5.3: Graphical representation of Gaussian-shaped landslides. In (a) different profiles are shown for different values of the parameters a and b . In (b) the instantaneous bathymetry $z = -\alpha x + p(x - x_0)$ is shown, where $x_0 = 2$ km, $a = 50.0$ m and $b = 500$ m. With respect to the following examples, it has been chosen a higher value of a for graphical purpose.

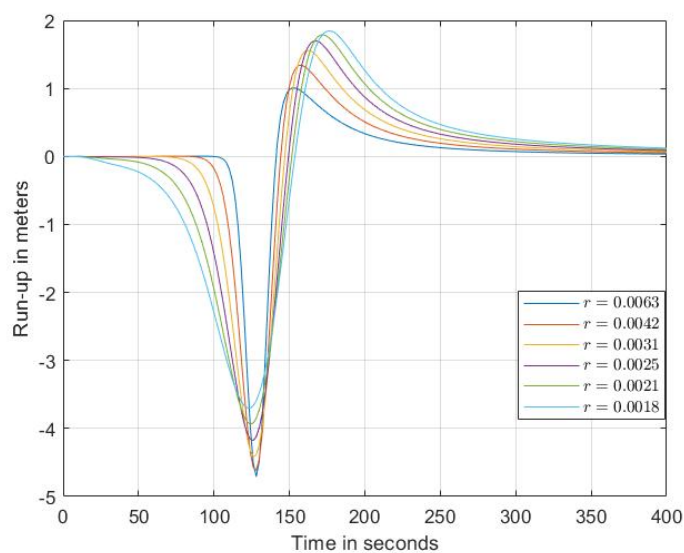
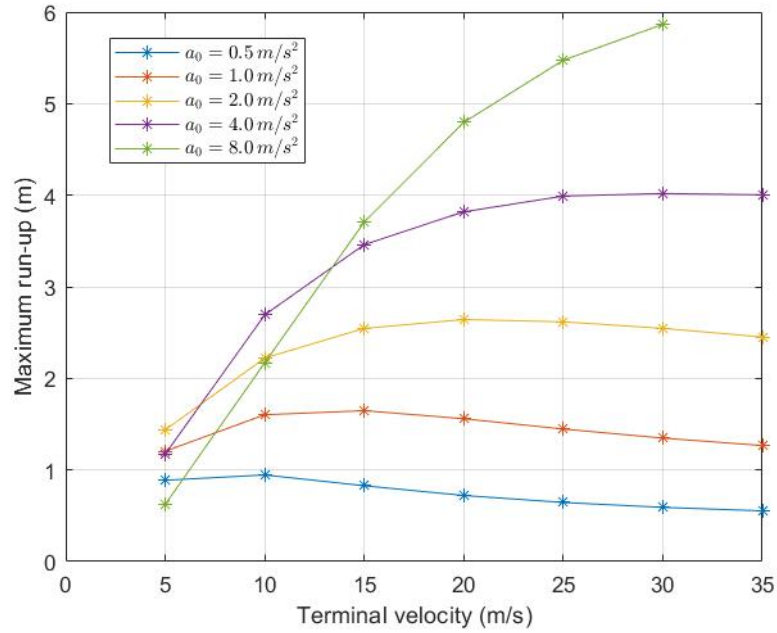
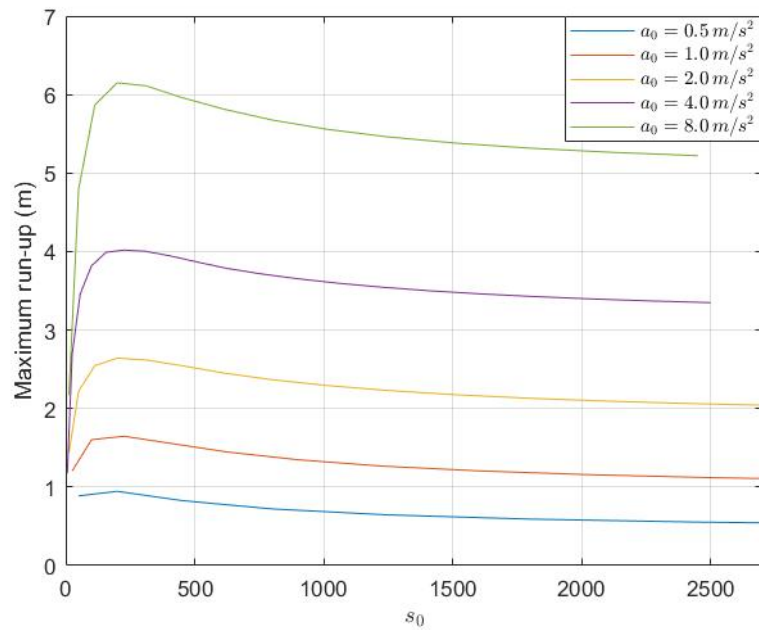


Figure 5.4: *Run-up function $R(t)$ for different aspect ratios. The parameters are chosen as follows: $a = 5.0$ m, $u_t = 10.0$ m s⁻¹, $a_0 = 1.0$ m/s², $x_0 = 2.0$ km, $\alpha = 0.05$ and b is calculated from a and r according to definition (5.9).*



(a)



(b)

Figure 5.5: Maximum run-up values for different values of the kinematic parameters a_0 and u_t . In (a) maximum run-up is calculated as a function of the terminal velocity u_t , while (b) shows the maximum run-up as a function of $s_0 = u_t^2/a_0$; in both plots, each curve corresponds to different values of the initial acceleration. The other parameters have been kept fixed: $a = 5.0 \text{ m}$, $b = 400 \text{ m}$, $x_0 = 2.0 \text{ km}$, $\alpha = 0.05$.

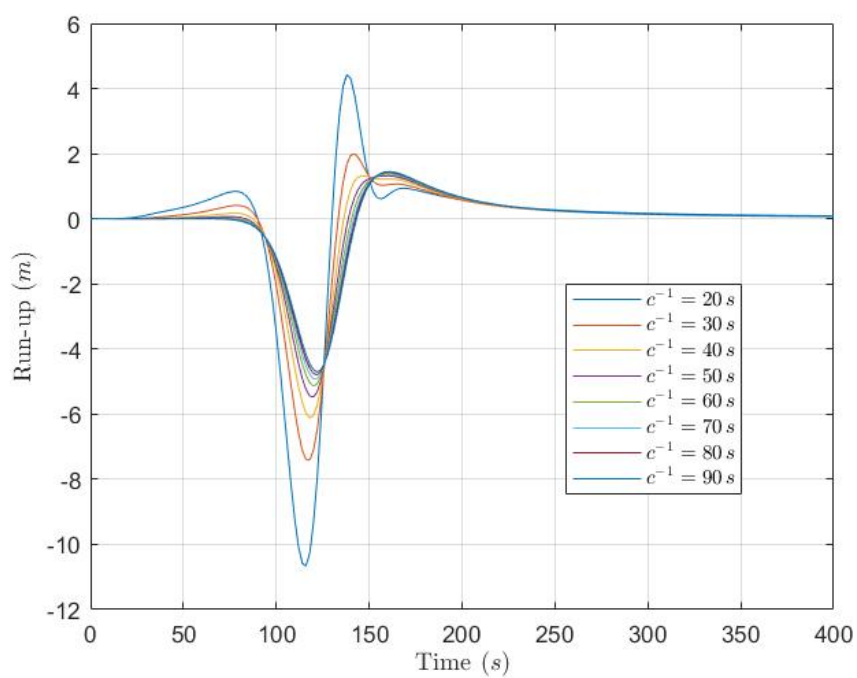


Figure 5.6: *Run-up functions for different values of c . The other parameters are fixed: $a = 5.0$ m, $b = 400$ m, $x_0 = 2.0$ km, $\alpha = 0.05$, $v_t = 20.0$ m s $^{-1}$, $a_0 = 1.0$ m/s 2 .*

Conclusion

Starting from a general linear solution for water wave evolution over a uniformly sloping bottom, a solution for the run-up function, i.e. for the shoreline motion, has been found. This solution is based on the representation of the ocean bottom deformation as superposition of sinusoidal functions with time-dependent amplitude and it only requires a fixed position domain, which means that the displacement in the origin and in an arbitrarily far point is assumed to be zero. Furthermore, contrary to many solutions based on the full nonlinear problem (Carrier & Greenspan (1958), Carrier et al. (2003), Tinti & Tonini (2005), Özeren & Postacioglu (2012)), this solution is very simple, in that it involves operations that very common in numerical problems, such as the calculation of Fourier coefficients, convolution integrals and derivatives, that acts only upon smooth functions, thus requiring no special care from the numerical point of view.

The applications illustrated in chapter 4 and 5 show the applicability of the model. First of all, both the cases of earthquake and landslide sources agree with analogous results that we may find in literature (e.g. Liu & Sepúlveda (2016) and Özeren & Postacioglu (2012) respectively). Secondly, examples of the versatility of the solution show that it may be used for numerical experiments. The purpose of such experiments may be the study of the dependence of the maximum run-up on parameters for which the functional relation is not obvious, such as the distance between the fault and the shoreline, or the prediction of run-up for precalculated scenarios in the context of early warning. **As an example, the scaling relation between maximum run-up and magnitude, based on the scaling relation by Wells & Coppersmith (1994) and**

the model presented, has been investigated.

From the previous chapter we may also conclude that, for the purpose of maximum run-up, a linear model is perfectly suitable and the complication of the full nonlinear problem may be ignored. This has been proved rigorously for the stationary points of initial value problems, but good agreement for the full run-up solution is found, both in the initial value problem (i.e. the earthquake case) and with time-dependent forcing (i.e. the landslide case). Thus, the major result of this work is the large applicability of the solution, as in the last example where it is applied to the a new simple model of landslide with time-dependent profile.

At last, we want to point the possible immediate generalizations that could be developed starting from here:

- other type of forcing may be investigated, in particular the cases of incoming incident waves and atmospheric perturbations, which have been here neglected, but they lead to a differential problem absolutely analogous to the linear shallow water equation solved here. This situation has already been studied in the context of wave generation, as by Pelinovsky et al. (2001);
- the problem could be generalized to a piecewise linear bathymetry, as it has been done for some nonlinear studies (see e.g. Synolakis (1987)). This case should allow to study jointly the effect of propagation, such as dispersion, and the run-up problem, as it has been done by Massel & Pelinovsky (2001);
- in some studies that concern mainly the generation of tsunami waves by underwater landslides, such as by Didenkulova et al. (2010), a transformation of variable in the wave equation is used in order to reduce the problem over an arbitrary bathymetry to the one with a flat ocean bottom. Similar approaches may be used in order to generalize the solution presented here to arbitrary analytical bathymetries, to account for any possible effect this could have.

Appendix A - Notes for the Numerical Implementation of the Solution

All results and graphs in this work have been obtained using MATLAB¹. The choice is mainly due to its simple and immediate syntax when it comes to numerical computation and the fact that numerical performance is not a concern for the present purpose. However, some precautions have to be taken.

In order to use the solution (3.29), we need as a starting point the definition of discretized domains for time t and position x . Central to this choice is the choice of the position domain length L : being a fixed boundary, the outgoing waves are reflected once they arrive at this extreme and may cause unphysical resonances. In the examples given in the work, the choice has been done empirically to obtain a time domain that shows the shoreline history before any artificial reflection enters the domain. As a rule of thumb, L has been taken about 10 times larger than the distance x_0 between the origin and the source. The domains are thus defined as the vectors $\{x_i\}_{i=0}^M$, with $x_0 = 0$, $x_M = L$ and the difference of consecutive elements is Δx , and $\{t_j\}_{j=0}^P$, with $t_0 = 0$, $t_P = T$ and the distance between consecutive elements is Δt . Once this is done, the source h_s can be defined as a matrix, where for example the element ij represents the vertical

¹For the MATLAB functions mentioned, the documentation in the MATLAB GUI and on the site mathworks.com are the best resources and many more examples and nuances can be found there.

displacements of the point x_i at time t_j .

The computation of the coefficients $\{A_n\}_{n=1}^N$ in (3.18) can be done analytically by the relation:

$$A_n = \frac{2}{L} \int_0^L h_s(q, t) \sin \frac{n\pi q}{L} dq$$

Since it is assumed that the function $h_s(x, t)$ is well-behaved, the computation is done using the *trapezoidal approximation*, using the function `y=trapz(x, z)`, which integrates the variable z over the domain x . The second derivative of the coefficients A_n is obtained by using `S(n)=4*diff(A(n), x)`, where x is the domain over which we differentiate.

The number of wave components has been chosen empirically. It is obvious that the further the source is from the centre of the domain, the bigger N has to be, for the properties of the trigonometric polynomials. Furthermore, the coseismic examples used are more complex, since they usually present a dipolar behaviour, while the Gaussian landslides are monopolar and thus we expect to need a large value of N for the seismic case. Throughout this work, $N = 2000$ has been used for the seismic examples, while $N = 600$ has been used for the landslide cases.

An issue one may encounter using MATLAB is the use of the Fresnel Integral functions, defined in (3.26). They are needed for the function $G(x)$ defined in (3.28), but are natively defined in MATLAB as symbolic object and their numerical use requires a few seconds each time they are called.. Since the function $G(x)$ has to be called approximately N times, a faster implementation may be useful. First we write the functions as

$$\begin{aligned} C\left(x\sqrt{\frac{\pi}{2}}\right) &= \frac{1}{2} + f(x) \sin\left(\frac{\pi}{2}x^2\right) - g(x) \cos\left(\frac{\pi}{2}x^2\right) \\ S\left(x\sqrt{\frac{\pi}{2}}\right) &= \frac{1}{2} - f(x) \cos\left(\frac{\pi}{2}x^2\right) - g(x) \sin\left(\frac{\pi}{2}x^2\right) \end{aligned}$$

and the functions $f(x)$ and $g(x)$ are approximated as

$$\begin{aligned} f(x) &\approx \frac{1 + 0.926x}{2 + 1.792x + 3.104x^2} + \epsilon(x) \\ g(x) &\approx \frac{1}{2 + 4.142x + 3.492x^2 + 6.67x^3} + \epsilon(x) \end{aligned}$$

where the error $\epsilon(x)$ is the error and is at the most 2×10^{-3} . This approximation from the NBS Handbook of Functions and others are discussed by Mielenz (1997).

The last thing we need to discuss is the convolution of causal functions, i.e. integrals in the form

$$y(t) = \int_0^t h(t')x(t-t')dt'$$

For the domain we are working on, the sampling period is Δt and we can write:

$$y(n\Delta t) = \sum_{i=0}^P \int_{i\Delta t}^{(i+1)\Delta t} h(t')x(n\Delta t - t')dt'$$

If Δt is small, the functions $h(t)$ and $x(t)$ may be assumed to be constant inside the each of the i -th intervals

$$y(n\Delta t) \simeq \sum_{i=0}^P h(i\Delta t)x(n\Delta t - i\Delta t) \int_{i\Delta t}^{(i+1)\Delta t} dt' = \sum_{i=0}^P h(i\Delta t)x(n\Delta t - i\Delta t)\Delta t$$

By using a discrete notation, the convolution can be computed as

$$y(n) = \sum_{i=0}^P h(i)x(n-i)\Delta t$$

The causality of the involved function means that whenever $n - i < 0$ the x is zero and we can write

$$y(n) = [h(0)x(n) + h(1)x(n-1) + \dots + h(n-1)x(1) + h(n)x(0)] \Delta t$$

that can be easily implemented using the function already implemented in MATLAB for splicing and dot product of vectors.

Bibliography

- [1] Ambraseys, N. N. (1962) Data for the investigation of the seismic sea-waves in the Eastern Mediterranean. *Bulletin of the Seismological Society of America*. 52 (4): 895–913.
- [2] Carrier, G., Greenspan, H. (1958). Water waves of finite amplitude on a sloping beach. *Journal of Fluid Mechanics*, 4(1), 97-109. doi:10.1017/S0022112058000331
- [3] Carrier, G., Wu, T., Yeh, H. (2003). Tsunami run-up and draw-down on a plane beach. *Journal of Fluid Mechanics*, 475, 79-99. doi:10.1017/S0022112002002653
- [4] Didenkulova, I., Nikolkina, I., Pelinovsky, E., Zahibo, N. (2010). Tsunami waves generated by submarine landslides of variable volume: Analytical solutions for a basin of variable depth. *Natural Hazards and Earth System Sciences*. 10. doi:10.5194/nhess-10-2407-2010.
- [5] Davies, B. (2002). *Integral Transforms and Their Applications*, Third Edition. Springer International Publishing, doi: 10.1007/978-1-4684-9283-5.
- [6] Fritz, H.M., Petroff, C.M., Catalán, P.A. et al. (2011). Field Survey of the 27 February 2010 Chile Tsunami. *Pure Appl. Geophys.* 168, 1989–2010, doi:10.1007/s00024-011-0283-5

- [7] Glimsdal, S., Pedersen, G., Harbitz, C., Løvholt, F., (2013). Dispersion of tsunamis: Does it really matter?. *Natural Hazards and Earth System Sciences*. 13. 1507-1526. doi:10.5194/nhess-13-1507-2013.
- [8] Grezio, A., Babeyko, A., Baptista, M. A., Behrens, J., Costa, A., Davies, G.,... Thio, H. K. (2017). Probabilistic Tsunami Hazard Analysis: Multiple sources and global applications. *Reviews of Geophysics*, 55, 1158– 1198. doi:10.1002/2017RG000579
- [9] Hanks, T. C., and Kanamori, H. (1979), A moment magnitude scale, *J. Geophys. Res.*, 84(B5), 2348– 2350, doi:10.1029/JB084iB05p02348.
- [10] Kajiura, K. (1963). Leading Wave of a Tsunami, *Bulletin Earthquake Research Institute*, Tokyo University, 41, 535-571.
- [11] Kundu, P.K., Cohen, I.M., Dowling, D.R. (2015). *Fluid Mechanics*, Sixth Edition. Elsevier Academic Press.
- [12] Levin, B. W., Nosov, M. (2016). *Physics of Tsunamis*, Second Edition. Springer International Publishing, doi:10.1007/978-3-319-24037-4.
- [13] Liu, P., Sepúlveda, I., (2016). Estimating tsunami runup with fault plane parameters, *Coastal Engineering*, 112, 57-68, doi:10.1016/j.coastaleng.2016.03.001.
- [14] Lorito, S., Tiberti, M. M., Basili, R., Piatanesi, A., and Valensise, G. (2008), Earthquake-generated tsunamis in the Mediterranean Sea: Scenarios of potential threats to Southern Italy, *J. Geophys. Res.*, 113, B01301, doi:10.1029/2007JB004943.
- [15] Massel, S., Pelinovsky, E., (2001). Run-up of dispersive and breaking waves on beaches. *Oceanologia*. 43. 61-97.
- [16] Maramai A., Brizuela B., Graziani L. (2014). The Euro-Mediterranean Tsunami Catalogue, *Annals of Geophysics*, 57, 4, S0435; doi:10.4401/ag-6437

- [17] Mori, N., Takahashi, T., Yasuda, T., and Yanagisawa, H. (2011), Survey of 2011 Tohoku earthquake tsunami inundation and run-up, *Geophys. Res. Lett.*, 38, L00G14, doi:10.1029/2011GL049210.
- [18] Murty, T. S., Loomis H. G., (1980). A new objective tsunami magnitude scale, *Marine Geodesy*, 4:3, 267-282, doi:10.1080/15210608009379388
- [19] Okada, Y., (1985). Surface deformation due to shear and tensile faults in a half-space. *Bulletin of the Seismological Society of America*; 75 (4): 1135–1154.
- [20] Omira, R., Dogan, G.G., Hidayat, R. et al. (2019) The September 28th, 2018, Tsunami In Palu-Sulawesi, Indonesia: A Post-Event Field Survey. *Pure Appl. Geophys.* 176, 1379–1395. doi:10.1007/s00024-019-02145-z
- [21] Özeren, M., Postacioglu, N. (2012). Nonlinear landslide tsunami run-up. *Journal of Fluid Mechanics*, 691, 440-460. doi:10.1017/jfm.2011.482
- [22] Pelinovsky, E., Poplavsky, A., (1996). Simplified model of tsunami generation by submarine landslides, *Physics and Chemistry of the Earth*, 21, 1–2, doi:10.1016/S0079-1946(97)00003-7
- [23] Pelinovsky, E., Talipova, T., Kurkin, A., Kharif, C. (2001). Nonlinear mechanism of tsunami wave generation by atmospheric disturbances. *Natural hazards and earth system sciences*. 1. doi:10.5194/nhess-1-243-2001.
- [24] Renzi, E., Sammarco, P. (2016). The hydrodynamics of landslide tsunamis: current analytical models and future research directions. *Landslides*. 13. doi:10.1007/s10346-016-0680-z.
- [25] Rybkin, A., Pelinovsky, E., Didenkulova, I., (2014). Nonlinear wave run-up in bays of arbitrary cross-section: generalization of the Carrier–Greenspan approach, *Journal of Fluid Mechanics*, 748, 416-432. doi:10.1017/jfm.2014.197

- [26] Saito, T., (2017). Tsunami generation: validity and limitations of conventional theories, *Geophysical Journal International*, 210-3, 1888–1900, doi:10.1093/gji/ggx275
- [27] Saito, T. (2019). *Tsunami Generation and Propagation*. Springer International Publishing, doi:10.1007/978-4-431-56850-6
- [28] Shearer, P. (2019). *Introduction to Seismology*, Third Edition. Cambridge University Press, doi:10.1017/9781316877111
- [29] Stirling, M., Goded, T., Berryman, K., Litchfield, N., (2013). Selection of Earthquake Scaling Relationships for Seismic-Hazard Analysis. *Bulletin of the Seismological Society of America*. 103 (6): 2993–3011. doi:10.1785/0120130052
- [30] Synolakis, C. (1987). The runup of solitary waves. *Journal of Fluid Mechanics*, 185, 523-545. doi:10.1017/S002211208700329X
- [31] Tinti, S., Bortolucci, E. (2000). Analytical Investigation on Tsunamis Generated by Submarine Slides. *Annali di Geofisica*, 43, 519-536, doi:10.4401/ag-3656.
- [32] Tinti, S., Bortolucci, E., Chiavettieri, C. Tsunami Excitation by Submarine Slides in Shallow-water Approximation. *Pure appl. geophys.* 158, 759–797 (2001). doi:10.1007/PL00001203
- [33] Tinti, S., Graziani, L., Brizuela, B., Maramai, A., Gallazzi, S.. (2012). Applicability of the Decision Matrix of North Eastern Atlantic, Mediterranean and connected seas Tsunami Warning System to the Italian tsunamis. *Natural Hazards and Earth System Sciences*. 12. 843-857. doi:10.5194/nhess-12-843-2012.
- [34] Tinti, S., Maramai, A. & Graziani, L. (2004). The New Catalogue of Italian Tsunamis. *Natural Hazards* 33, 439–465. doi:10.1023/B:NHAZ.0000048469.51059.65
- [35] Tinti, S., Tonini, R. (2005). Analytical evolution of tsunamis induced by near-shore earthquakes on a constant-slope ocean. *Journal of Fluid Mechanics*, 535, 33-64. doi:10.1017/S0022112005004532

- [36] Tinti, S., Tonini, R., (2013). The UBO-TSUFDF tsunami inundation model: Validation and application to a tsunami case study focused on the city of Catania, Italy. *Natural Hazards and Earth System Sciences*. 13. 1795-1816. doi:10.5194/nhess-13-1795-2013.
- [37] Tinti, S., Tonini, R., Bressan, L., Armigliato, A., Gardi, A., Guillaude, R., Valencia, N. & Scheer, S., (2011). Handbook of Tsunami Hazard and Damage Scenarios. *JRC Scientific and Technical Reports*.
- [38] Tuck, E., Hwang, L. (1972). Long wave generation on a sloping beach. *Journal of Fluid Mechanics*, 51(3), 449-461. doi:10.1017/S0022112072002289
- [39] Udías, A., Buforn, E. (2018). *Principles of Seismology*, Second Edition. Cambridge University Press, doi:10.1017/9781316481615
- [40] Watts, P. (1997) *Water waves generated by underwater landslides*. Dissertation (Ph.D.), California Institute of Technology. doi:10.7907/S3NH-RA23.
- [41] Wells, D., Coppersmith, K., (1994). New empirical relationships among magnitude, rupture length, rupture width, rupture area, and surface displacement. *Bulletin of the Seismological Society of America*. 84 (4): 974–1002.
- [42] Zengaffinen, T., Løvholt, F., Pedersen, G. et al. (2020). Modelling 2018 Anak Krakatoa Flank Collapse and Tsunami: Effect of Landslide Failure Mechanism and Dynamics on Tsunami Generation. *Pure Appl. Geophys.* 177, 2493–2516, doi:10.1007/s00024-020-02489-x